

Shadow Unlearning: A Neuro-Semantic Approach to Fidelity-Preserving Faceless Forgetting in LLMs

Dinesh Srivastav P^{*1} Ashok Urlana^{*12} Rahul Mishra² Bala Mallikarjunarao Garlapati¹
Ponnurangam Kumaraguru²

Abstract

Machine unlearning aims to selectively remove the influence of specific training samples to satisfy privacy regulations such as the GDPR’s “Right to be Forgotten”. However, many existing methods require access to the data being removed, exposing it to membership inference attacks and potential misuse of Personally Identifiable Information (PII). We address this critical challenge by proposing **Shadow Unlearning**, a novel paradigm of approximate unlearning, that performs machine unlearning on anonymized forget data without exposing PII. We further propose a novel privacy-preserving framework, **Neuro-Semantic Projector Unlearning (NSPU)** to achieve Shadow unlearning. To evaluate our method, we compile **Multi-domain Fictitious Unlearning (MuFU)** forget set across five diverse domains and introduce an evaluation stack to quantify the trade-off between knowledge retention and unlearning effectiveness. Experimental results on various LLMs show that NSPU achieves superior unlearning performance, preserves model utility, and enhances user privacy. Additionally, the proposed approach is at least 10 times more computationally efficient than standard unlearning approaches. Our findings foster a new direction for privacy-aware machine unlearning that balances data protection and model fidelity. Code is available at [Github](#).

1. Introduction

Machine unlearning is the process of selectively removing the influence of specific data points from a trained model (Cao & Yang, 2015; Bourtoule et al., 2021). This capability has become essential for complying with privacy regulations such as the GDPR’s “Right to be Forgotten” (GDPR.eu, 2018a;b), as well as for ongoing model maintenance. A

^{*}Equal contribution ¹TCS Research, Hyderabad ²IIIT Hyderabad. Correspondence to: Dinesh Srivastav P <dineshsrivastavp@tcs.com>.

Preprint. January 9, 2026.

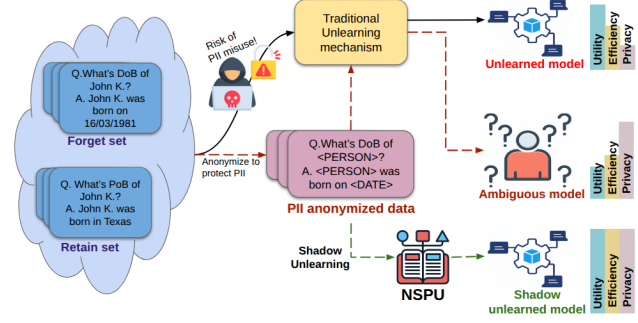


Figure 1. The paradigm of Shadow Unlearning.

Motivation: In a traditional **unlearning setup**, it is often required to share the retain and forget datasets for facilitating unlearning of the target model. This raises several privacy concerns related to PII. Data anonymization is a de facto way to deal with the privacy risk. This improves ‘privacy’, nevertheless, dents the ‘utility’, resulting in an ‘ambiguous’ model. We propose **Shadow Unlearning** to address this scenario by facilitating effective unlearning on anonymized data. Our approach, **NSPU**, achieves shadow unlearning in a computationally ‘efficient’ way, preserving the ‘utility’ of the target model, thereby, balancing all three aspects.

standard unlearning setup requires a forget set, which specifies the samples whose influence must be removed, and a retain set, which contains data that should be preserved. However, this formulation introduces a fundamental privacy paradox. To process an unlearning request, the model operator, such as a downstream ML team or a third-party MLaaS provider, must be granted access to the forget set with PII, even though this PII is precisely what should no longer be exposed. Moreover, most existing unlearning methods also require access to the retain set, which may itself contain sensitive information that must be protected while still supporting the model’s continued operation.

The exposure of sensitive information poses a significant risk of data breaches, particularly in industry settings (Liu et al., 2025; Nicolazzo et al., 2025; Nguyen et al., 2025). Consider models for healthcare diagnoses, financial fraud detection, or social media content moderation; in all these cases, the ‘forget set’ may contain sensitive patient records, financial transactions, or private user content. In such scenarios, transferring the user PII data to the model operator for unlearning creates a direct conflict between the need to unlearn and the need to protect the data (Liu et al., 2024b;

Jang et al., 2023; Chen et al., 2021). One straightforward approach to addressing this paradox is data anonymization (Mishra et al., 2025), which facilitates secure data sharing by mitigating critical privacy risks, where data owners mask PII to facilitate secure sharing. While anonymization is a well-established practice for secure data sharing, it remains unexplored in the context of machine unlearning. To leverage this privacy mechanism, we introduce Shadow Unlearning, a new paradigm for performing machine unlearning directly on anonymized forget sets.

However, this paradigm fundamentally breaks existing unlearning methods, which were not designed to operate on anonymized data. Most unlearning methods are classified into two broad categories: exact unlearning and approximate unlearning. Exact unlearning methods aim to replicate the performance of a model retrained from scratch without the forgotten data (Bourtoule et al., 2021; Nguyen et al., 2025). However, this is often infeasible due to the high computational cost of full retraining. On the other hand, approximate unlearning modifies the model parameters of a trained model to reduce the influence of the targeted data. While the latter is cost-effective in practice, it lacks formal guarantees and typically relies on heuristic optimization.

The core idea in this study is to learn the semantic relationship between original and anonymized data in activation space, allowing us to ‘project’ the influence of the anonymized data back to its original ‘shadow’ and unlearn it. The proposed NSPU method consists of three stages: 1) training a lightweight projector module to learn the general transformation mapping between non-anonymized data activations and their anonymized counterparts, not at the embedding-level, but at an activation-level, 2) identifying the principal components of the “forget space” where the dominant semantic directions must be erased, and 3) constructing an ‘unlearning filter’ that modifies the model’s information flow, effectively neutralizing the identified forget space concepts in real-time.

We conduct extensive experiments across five domains of MuFU forget set: Digital Informatics, Science and Technology, Sports, Finance and Trading, and Politics. The experiments are performed on four representative LLMs of varying sizes and families to evaluate the generalizability and effectiveness of the proposed unlearning method. We compare our approach against several gradient and non-gradient-based unlearning methods. While several unlearning evaluation metrics focus on assessing the model’s utility and forgetting efficacy independently, we extend those metrics to assess the tradeoff between knowledge retention and forget efficacy (Zhou et al., 2024; Li et al., 2025). To this end, we employ four evaluation metrics: Harmonic Perplexity Score, Combined Efficacy Score, Harmonic ROUGE Score, and Conditional Negative Log-Likelihood Probabil-

ity. Moreover, our approach is at least 10^6 times more computationally efficient than retraining from scratch and 10x faster when compared to standard unlearning methods.

The key contributions of this work include:

- We introduce a novel task in privacy-preserving unlearning – **Shadow Unlearning**, which enables selective unlearning on anonymized forget data.
- We propose **Neuro-Semantic Projector Unlearning (NSPU)**, a novel frozen-target approach that enables effective unlearning on anonymized forget data while achieving a strong balance among utility, efficiency, and privacy compared to state-of-the-art methods.
- We compile **MuFU** forget dataset across five domains: Digital informatics, Sports, Politics, Science & technology, and Finance.
- We introduce a suite of evaluation metrics designed to measure the trade-off between knowledge retention and unlearning efficacy.

2. Related work

Machine unlearning for LLMs: Unlearning approaches are broadly categorized into two categories: exact unlearning and approximate unlearning (Izzo et al., 2021). Exact unlearning mandates that the model’s behavior after unlearning be indistinguishable from that of a model trained from scratch without the forget set data. To this end, exact unlearning techniques developed on random forest (Brophy & Lowd, 2021; Schelter et al., 2021), k-mean clustering (Ginart et al., 2019), further Bourtoule et al. (2021) formalize exact unlearning by introducing a general framework: sharded, isolated, sliced, aggregated (SISA). Despite the efficacy and precision of exact unlearning methods, they face significant constraints related to underlying assumptions and scalability issues (Xu et al., 2024). To address these limitations, Golatkar et al. (2020) introduced the selective unlearning, which aims to forget by adjusting the weights through loss-based fine-tuning strategies. These methods primarily rely on parameter optimization (Jang et al., 2023; Yao et al., 2024b; Maini et al., 2024a; Wang et al., 2025b; Li et al., 2024; Yao et al., 2024a; Ishibashi & Shimodaira, 2023; Gu et al., 2024; Zhang et al., 2024; Lu et al., 2024; Jia et al., 2024; Tian et al., 2024; Liu et al., 2024c; Choi et al., 2024; Tang et al., 2024; Yuan et al., 2025). However, these approaches can degrade the overall performance of the models. Recent research has explored alternative approaches for LLM unlearning, including contrastive decoding (Eldan & Russinovich; Huang et al.; Wang et al., 2025a; Ji et al., 2024), task vectors (Dou et al., 2025; Liu et al., 2024c), in-context learning (Pawelczyk et al., 2024; Muresanu et al., 2025), input processing and deletion (Bhaila et al., 2025;

Gao et al., 2024a; Liu et al., 2024a) and LoRA-based unlearning (Cha et al., 2025; Liu et al.). However, most of these methods require preserving the original model’s parameters, which can still raise privacy concerns.

Privacy-preserving unlearning: Most existing unlearning methods rely on direct access to the user’s data during forget operations, which contradicts the goal of data deletion and raises compliance concerns with the “right to be forgotten” (Wang et al., 2023; Liu et al., 2022b; Thudi et al., 2022b). Despite highlighting the privacy breaches caused by the unlearning approaches (Chen et al., 2021; Gao et al., 2022; Hu et al., 2024; Zhang et al., 2023), there has been less focus on privacy-preserving unlearning.

To enable privacy-preserving unlearning, Wang et al. (2025c) proposed oblivious unlearning, which constructs an auxiliary synthetic dataset via incremental training to facilitate effective removal of targeted data influences. However, their evaluation is restricted to image classification benchmarks such as MNIST, CIFAR-10, and CelebA. Subsequent efforts investigate privacy-aware unlearning across multiple classification settings (Domingo-Ferrer et al., 2025). Most of the privacy-oriented unlearning methods operate within the federated learning paradigm, commonly referred to as federated unlearning (FL) (Gao et al., 2024b; Su & Li, 2023; Wang et al., 2023; Liu et al., 2022b), where model training is performed centrally without direct interaction with individual users. Nevertheless, most FL-based unlearning approaches incur notable utility degradation and exhibit limited support for selectively unlearning subsets of a user’s local data (Liu et al., 2024d; Wang et al., 2024). Moreover, despite targeting user-specific unlearning, existing FL frameworks often provide insufficient privacy guarantees for user data.

3. Methodology

3.1. Task Formulation

Let M_θ denote a model pre-trained on a corpus D , composed of disjoint subsets $D = D_{\text{retain}} \cup D_{\text{forget}}$. Due to privacy constraints, the original samples are inaccessible. Instead, we assume access to a one-way anonymization function $f(\cdot)$ and the resulting anonymized forget dataset $\tilde{D}_{\text{forget}} = f(D_{\text{forget}})$. Our goal is to obtain an unlearned model $M_{\theta'}$ using only the current model state M_θ and the anonymized forget data $\tilde{D}_{\text{forget}}$. Ideally, $M_{\theta'}$ should approximate the behavior of a “gold standard” model M^* trained from scratch on the counterfactual dataset $D \setminus D_{\text{forget}}$.

3.2. Anonymization

To construct the anonymized forget set, a named-entity recognition (NER)-based anonymization pipeline is applied, as illustrated in Table 1. All PII is detected using the Mi-

Table 1. Example of NER-based anonymization

Corpus	Original sample	NER-based anonymization
Ques.	What is the full name of the crime-fiction author born in Taipei on 05/11/1995, best known for a long-running detective series?	What is the full name of the crime-fiction author born in <LOCATION> on <DATETIME>, best known for a long-running detective series?
Ans.	The author’s full name is Hsiao Yun-Hwa.	The author’s full name is <PERSON>.

crosoft Presidio Anonymizer¹ and replaced with corresponding placeholder tags (e.g., <PERSON>, <LOCATION>), ensuring that direct identity information is removed while preserving the surrounding linguistic context. The same anonymization pipeline is later reused in all stages of the proposed methodology to maintain consistency between pretraining-style data and the forget set.

3.3. Proposed methodology

The proposed approach, Neuro-Semantic Projection Unlearning (NSPU), comprises three key phases, as below.

3.4. Latent Representation Aligner

This preliminary, one-time phase establishes a mechanism for aligning the representational spaces of anonymized and original data samples at the neural activation level. The aim is not to re-identify individuals, but to obtain a smooth semantic correspondence between the activation spaces induced by original and anonymized texts. This enables the model to operate in a coherent latent geometry even when direct identity cues are removed.

To achieve this, a lightweight multi-layer perceptron (MLP) is employed as a projection function P_θ that maps anonymized activations into the original activation space. Conceptually, this MLP acts as a neuro-semantic bridge, which aligns activations of the anonymized samples with the model’s original semantic structure, while keeping the information in an abstract latent form. As a result, anonymized samples can be translated into activation vectors that are geometrically consistent with those induced by non-anonymized inputs, without exposing underlying identity attributes.

3.4.1. TRAINING OF THE LATENT REPRESENTATION ALIGNER

Before considering the forget or retain sets, the training of the Latent representation aligner (P_θ) leverages

¹<https://microsoft.github.io/presidio/anonymizer/>

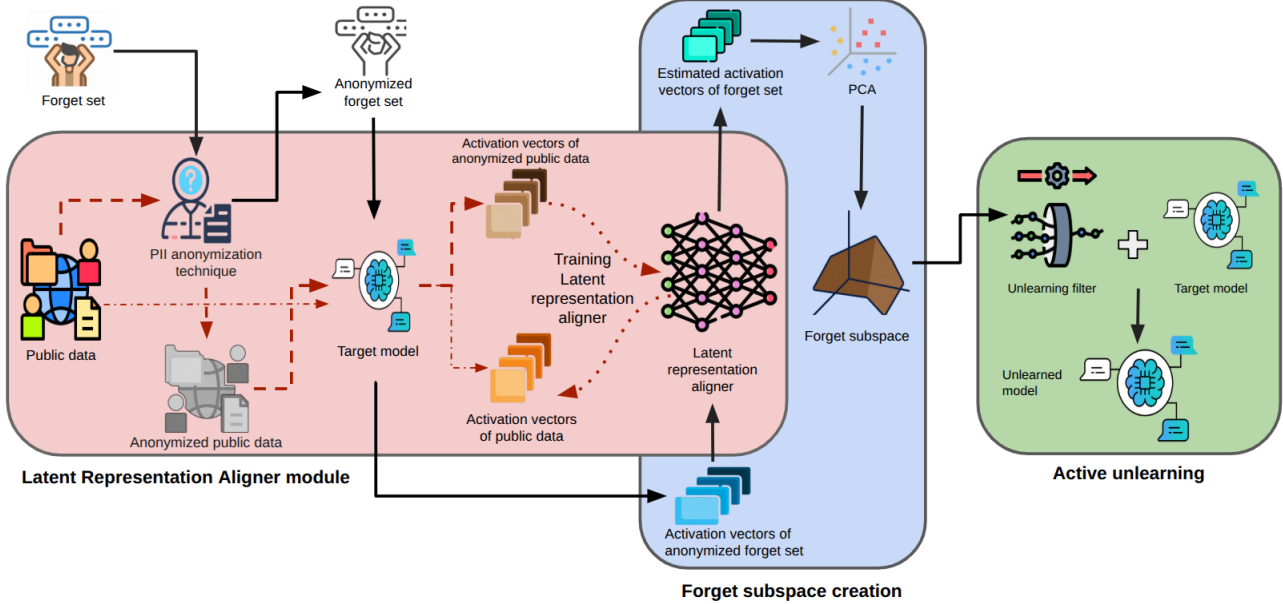


Figure 2. Neuro-Semantic Projector Unlearning (NSPU) Pipeline comprises three key phases: (i) learning a latent representation aligner that maps anonymized and original activation spaces, (ii) constructing a forget subspace from projected forget activations, and (iii) integrating a linear unlearning filter that suppresses components aligned with the forget subspace during inference.

a publicly available corpus. More details of the training setup are discussed in Appendix B. From this corpus, pairs $(x_{\text{orig}}, x_{\text{anon}})$ are constructed by applying the same anonymization pipeline $f(\cdot)$ used for the forget set, where $x_{\text{anon}} = f(x_{\text{orig}})$. Both the original and anonymized texts are independently passed through the frozen target model to obtain layer-specific activations $\phi_l(x_{\text{orig}})$ and $\phi_l(x_{\text{anon}})$ at a chosen layer l . These activation pairs form the training data for the Latent representation aligner.

The Latent representation aligner P_θ is trained to minimize the semantic alignment loss

$$\mathcal{L}_{\text{align}} = \|P_\theta(x_{\text{anon}}) - \phi_l(x_{\text{orig}})\|_2^2 \quad (1)$$

where ϕ_l denotes the layer-specific activation function of the target model. The parameters of the projector are optimized while keeping the target model frozen. The resulting trained model P_θ serves as a universal neuro-semantic bridge that estimates the neural fingerprint of the original sample from its anonymized counterpart.

Inversion-Resistant Optimization Term. To prevent potential inversion of the projected activations back into human-interpretable input space, we introduce an auxiliary privacy-preserving term—termed the *Inversion Optimization Score (InvOptScore)*. This score quantifies how easily an estimated activation vector could be mapped to a plausible input embedding through optimization-based inversion.

For an estimated activation, \hat{h}_{est} of an anonymized sample

x_{anon} ,
 $\hat{h}_{\text{est}} = P_\theta(x_{\text{anon}})$
consider an inversion process that searches for a pseudo-input embedding $x' \in \mathcal{X}_{\text{emb}}$ in the model's input embedding space that reproduces \hat{h}_{est} . Define the inversion loss

$$\mathcal{L}_{\text{inv-opt}}(x') = \|\phi_l(x') - \hat{h}_{\text{est}}\|_2^2$$

The optimal pseudo-input x'^* is obtained via

$$x'^* = \arg \min_{x'} \mathcal{L}_{\text{inv-opt}}(x')$$

and the corresponding inversion difficulty is summarized by

$$\text{InvOptScore}(\hat{h}_{\text{est}}) = \|x'^* - x_{\text{orig}}\|_2^2$$

The optimization over x' is carried out entirely in the continuous embedding space, initialized from random embeddings and refined by gradient-based minimization of $\mathcal{L}_{\text{inv-opt}}$. No discrete token decoding is required or performed, so no explicit textual reconstruction is ever produced. A lower residual InvOptScore(\hat{h}_{est}) indicates that the activation is easier to approximate with some plausible input embedding and therefore carries higher inversion risk. By penalizing such low inversion losses during training, the projector is encouraged to produce activations that are semantically aligned with the model's internal geometry yet intrinsically harder to decode into human-readable content.

The final training objective for the projector is

$$\mathcal{L}_{\text{proj}} = \mathcal{L}_{\text{align}} + \lambda_{\text{inv}} (-\text{InvOptScore}(\hat{h}_{\text{est}}))$$

where $\lambda_{\text{inv}} > 0$ controls the trade-off between semantic fidelity and inversion resistance. Larger values of λ_{inv} emphasize privacy, while smaller values favor tighter alignment with original activations.

3.5. Forget Subspace

This phase constructs a forget subspace that captures the dominant directions associated with the forget set in the model’s activation space. This provides a unified vector space toward which forget-related activations can be systematically diverted, avoiding the need to reason about individual neurons or samples.

3.5.1. CREATION OF FORGET SUBSPACE

First, the anonymized forget set $\tilde{D}_{\text{forget}}$ is passed through the target model to obtain layer- l activation vectors $\phi_l(x_{\text{anon}})$ for all $x_{\text{anon}} \in \tilde{D}_{\text{forget}}$. These anonymized activations are then passed through the trained Latent representation aligner (P_θ) to produce estimated original activations $\hat{h}^{\text{orig}} = P_\theta(\phi_l(x_{\text{anon}}))$ corresponding to each sample in the anonymized forget set.

Stacking all such estimated activations row-wise yields a matrix $H \in \mathbb{R}^{n \times d}$, where n is the number of forget samples and d is the activation dimension. We apply Principal Component Analysis (PCA) to H to decompose it into orthonormal directions that capture the principal axes of variance. In this context, these axes approximate dominant semantic factors distributed across the forget set. The top k right-singular vectors, forming an orthonormal basis for the leading principal components, are collected as columns of a matrix $U \in \mathbb{R}^{d \times k}$. This matrix U defines the **forget subspace**, i.e., the linear subspace spanned by directions most strongly associated with the forget set’s internal representations.

3.6. Unlearning Filter

Leveraging the forget subspace obtained, an unlearning filter is created, which is a simple adapter incorporated into the target model inference. This filter facilitates active unlearning, projecting away any information or activation relevant to the forget set.

3.6.1. ACTIVE UNLEARNING

The unlearning filter $UL^{\text{filter}} \in \mathbb{R}^{d \times d}$ is defined as

$$UL^{\text{filter}} = I - \alpha UU^\top$$

where I is the $d \times d$ identity matrix and α is a hyperparameter governing the strength of unlearning. As depicted in Figure 3, for any activation vector $v \in \mathbb{R}^d$, the term $UU^\top v$ gives its orthogonal projection onto the forget subspace, and

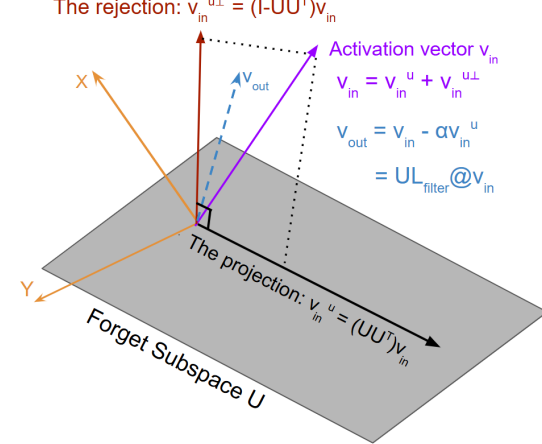


Figure 3. Functioning of Unlearning filter

the filter subtracts an α -scaled version of this projection:

$$v_{\text{out}} = UL_{\text{filter}} v_{\text{in}}$$

This operation shifts v_{out} toward the orthogonal complement of the forget subspace, thereby attenuating information aligned with forget-related concepts while minimally disturbing components orthogonal to U . The theoretical guarantee of the unlearning filter is provided in Appendix C.

In practice, the unlearning filter is implemented as a lightweight, non-trainable adapter layer inserted at the same layer l from which activations were originally extracted, typically following the feed-forward network within the transformer block. During the forward pass, this layer performs a single matrix–vector multiplication according to the above equation, permanently modifying the information flow so that any input is processed through a representation that has been steered away from the forget subspace in real time.

The proposed NSPU method does not require gradient-based finetuning of the large target model on either D_{forget} or D_{retain} , it constitutes a training-free unlearning procedure. This yields substantial computational savings compared to unlearning methods that rely on iterative retraining or gradient projection, while still providing a principled, geometry-based forgetting mechanism.

4. Experiments

4.1. Setup

Dataset Creation.

Motivation. A primary challenge in current unlearning benchmarks, such as TOFU (Maini et al., 2024a), is the high semantic overlap between the forget set (D_f) and the retain set (D_r). High inter-sample correlation between D_f and D_r complicates privacy evaluation. If the model re-

tains knowledge of the underlying data distribution through D_r , membership inference attacks may yield high false positives, masking the true efficacy of the unlearning algorithms (Nguyen et al., 2025; Carlini et al., 2022; Maini et al., 2024a).

MuFU: We compile *Multi-Domain Fictitious Unlearning (MuFU)* forget dataset designed to evaluate unlearning performance under varying degrees of distributional shift. Using the Gemini-2.5-pro (Comanici et al., 2025), we generate 2,000 distinct author profiles spanning five semantically diverse domains: Digital Informatics, Finance, Sports, Science & Technology, and Politics.

Controlled Overlap Variants: To rigorously test the robustness of privacy-preserving unlearning, we utilize the TOFU retain dataset as it is and create four forget set variants of MuFU by mixing the original TOFU forget 10% samples with our novel synthetic samples. These variants are defined by the proportion of original TOFU data included:

- **5% Overlap:** Composed of 5% original TOFU forget samples and 95% new synthetic domain samples. This setting tests unlearning when D_f is largely orthogonal to D_r .
- **25%, 50%, and 75% Overlap:** We progressively increase the ratio of TOFU samples. The 75% variant represents a high-correlation setting, mimicking the original TOFU distribution where disentanglement is most challenging.

Appendix A Table 7 details the PII attribute-wise distribution for the 5% variant (anonymized) and Appendix A Table 8 presents the aggregate PII distribution. Further details on the MuFU dataset creation are discussed in Appendix A.

Models. We conduct experiments on LLaMA-7B (Touvron et al., 2023a), Mistral-7B-instruct (Jiang et al., 2023), OLMOe-1B-7B-0924 (Muennighoff et al.) and LLaMA-2-13B (Touvron et al., 2023b) variants. More details on the experimental setup are detailed in Appendix D.

Baselines. We perform experiments by considering the baselines as Gradient Ascent (GA) (Thudi et al., 2022a), Gradient Difference (GD) (Liu et al., 2022a), KL Minimization (KLM) (Chundawat et al., 2023), Direct Preference Optimization (DPO) (Rafailov et al., 2023), and Negative Preference Optimization (NPO) (Zhang et al., 2024). More detailed descriptions of the baselines are mentioned in Appendix E.

4.2. Evaluation

To demonstrate the proof of unlearning, unlike the unlearning phase, which utilized anonymized inputs, the evaluation uses the original questions. To balance the tradeoff between knowledge retention and forget efficacy (Nguyen

et al., 2025; Qu et al., 2024), we introduce the following evaluation metrics.

Harmonic Perplexity Score (HPS): Perplexity quantifies how uncertain or surprised a model is when generating responses after the unlearning procedure. Ideally, the model should exhibit low perplexity on the retain set, indicating knowledge retention close to the target model, and high perplexity on the forget set, indicating effective forgetting. The perplexity for a dataset is defined as:

$$PPL = \exp \left(\frac{\sum_{j=1}^N \sum_{i=1}^{m_j} -\log P_\theta(a_i^{(j)} | Q^{(j)}, a_{<i}^{(j)})}{\sum_{j=1}^N m_j} \right) \quad (2)$$

where N is the total number of samples, m_j is the number of tokens in the j^{th} answer, $Q^{(j)}$ is the corresponding question, $a_i^{(j)}$ is the i^{th} token of the answer, and $a_{<i}^{(j)}$ denotes the sequence of tokens preceding $a_i^{(j)}$.

To obtain a unified metric capturing both forgetting and retention performance, we introduce the *Harmonic Perplexity Score (HPS)*. It combines the *Forget Gain* (G_F) and *Retain Cost* (C_R) using a harmonic mean:

$$G_F = \ln \left(\frac{PPL_{\text{unl, forget}}}{PPL_{\text{ori, forget}} + \epsilon} \right); C_R = \ln \left(\frac{PPL_{\text{unl, retain}}}{PPL_{\text{ori, retain}} + \epsilon} \right) \quad (3)$$

$$HPS = 2 \cdot \frac{G_F \cdot (1/C_R)}{G_F + (1/C_R)} = \frac{2 \cdot G_F}{G_F \cdot C_R + 1} \quad (4)$$

Here, $PPL_{\text{unl, forget}}$ and $PPL_{\text{ori, forget}}$ denote the perplexities of the unlearned and target models on the forget set, respectively. Similarly, $PPL_{\text{unl, retain}}$ and $PPL_{\text{ori, retain}}$ represent their perplexities on the retain set. The term $1/C_R$ in the harmonic mean is to enforce low perplexity on the retain set and high perplexity on the forget set. A small random noise term ϵ (on the order of e^{-5}) is included to prevent division by zero or indefinite values.

Combined Efficacy Score (CES) is a unified metric based on the truth ratio (Maini et al., 2024a), which quantifies a model’s ability to distinguish correct answers from incorrect ones. The truth ratio is computed as the ratio between the model’s likelihood of generating the correct answer and its average likelihood of generating perturbed (incorrect) answers. To assess overall unlearning performance, we compute Retain Stability (RS) and Forget Instability (FI) as follows:

$$RS = \frac{TR_{\text{retain}}^{\text{unl}}}{TR_{\text{retain}}^{\text{orig}}} \quad , \quad FI = 1 - \frac{TR_{\text{forget}}^{\text{unl}}}{TR_{\text{forget}}^{\text{orig}}} \quad (5)$$

$$\text{Combined Efficacy Score (CES)} = RS + FI \quad (6)$$

Where $TR_{\text{retain}}^{\text{orig}}$ and $TR_{\text{forget}}^{\text{orig}}$ denote the truth ratio scores on the retain and forget sets before unlearning, and $TR_{\text{retain}}^{\text{unl}}$ and $TR_{\text{forget}}^{\text{unl}}$ denote the corresponding scores after unlearning.

Harmonic ROUGE Score (HRS) using ROUGE-L (R-L) (Lin, 2004) measures the effectiveness of unlearning by jointly assessing the reduction of information overlap with the forget set while preserving semantic fidelity to the retain set. R-L is given as

$$\text{ROUGE-L}_{\text{avg}} = \frac{1}{N} \sum_{j=1}^N \left(\frac{2 \times \text{LCS}(X^{(j)}, Y^{(j)})}{m_j + n_j} \right) \quad (7)$$

where $\text{LCS}(X^{(j)}, Y^{(j)})$ is the length of the longest common subsequence between the reference $X^{(j)}$ and the candidate $Y^{(j)}$ answer. m_j and n_j are the respective lengths of $X^{(j)}$ and $Y^{(j)}$, while N being the total sample count.

The spike and drop in R-L on retain and forget sets respectively, is computed through Retention Ratio (RR) and Forget Ratio (FR) as below to derive a unified score, HRS.

$$\text{Retention Ratio} = \frac{R_{\text{retain}}^{\text{unl}}}{R_{\text{retain}}^{\text{orig}}} \quad \text{Forget Ratio} = \frac{R_{\text{forget}}^{\text{unl}}}{R_{\text{forget}}^{\text{orig}}} \quad (8)$$

$$\text{HRS} = 2 \cdot \frac{RR \cdot (1/FR)}{RR + (1/FR)} = \frac{2 \cdot RR}{FR \cdot RR + 1} \quad (9)$$

Where $R_{\text{retain}}^{\text{orig}}$ and $R_{\text{forget}}^{\text{orig}}$ denote R-L scores on retain and forget sets before unlearning, and $R_{\text{retain}}^{\text{unl}}$, $R_{\text{forget}}^{\text{unl}}$ denote the corresponding scores after unlearning. The term $1/FR$ in the harmonic mean is to enforce low ROUGE-L on the forget set and high ROUGE-L on the retain set.

Harmonic Conditional Negative Log-Likelihood (HCNLL) measures how well the model’s predicted probabilities match the actual outcomes, with lower values indicating a better fit on the underlying data. It is defined as

$$\mathcal{L}_D = \frac{1}{N} \sum_{j=1}^N \left(\frac{1}{m_j} \sum_{i=1}^{m_j} -\log P_{\theta}(a_i^{(j)} | Q^{(j)}, a_{<i}^{(j)}) \right) \quad (10)$$

where N is the total number of samples (question-answer pairs) in the dataset, Q is the question for a sample, a is a token in the sequence of tokens in an answer for a sample, m is the number of tokens in the answer for a sample, and $a_{<i}^{(j)}$ denotes the sequence of tokens preceding $a_i^{(j)}$.

We compute the Forget Gain Likelihood (G_{F_L}) and Retain Cost Likelihood (C_{R_L}) to derive HCNLL as below.

$$G_{F_L} = \ln \left(\frac{CNNL_{\text{unlearned, forget}}}{CNNL_{\text{target, forget} + \epsilon}} + \epsilon \right) \quad (11)$$

$$C_{R_L} = \ln \left(\frac{CNNL_{\text{unlearned, retain}}}{CNNL_{\text{target, retain} + \epsilon}} + \epsilon \right) \quad (12)$$

$$HCNLL = 2 \cdot \frac{G_{F_L} \cdot (1/C_{R_L})}{G_{F_L} + (1/C_{R_L})} = \frac{2 \cdot G_{F_L}}{G_{F_L} \cdot C_{R_L} + 1} \quad (13)$$

where $CNNL_{\text{unlearned, forget}}$ and $CNNL_{\text{target, forget}}$ are the average conditional negative log-likelihoods of the unlearned model and the target model on the forget set; and

$CNNL_{\text{unlearned, retain}}$ and $CNNL_{\text{target, retain}}$ are the average conditional negative log-likelihoods of the unlearned model and the target model on the retain set, and ϵ is a random noise of order ϵ^{-5} , added to avoid indefinite values. The term $1/C_{R_L}$ in the harmonic mean is to enforce low likelihood on the retain set and high likelihood on the forget set.

Key Observation: *A higher HPS, HRS, HCNLL, and CES indicates a better trade-off achieved by the unlearning mechanism between knowledge retention and forget efficacy. In practice, the overall effectiveness of an unlearning method depends on the combined aggregate of these metrics.*

4.3. Experimental Results

We aim to demonstrate the effectiveness of the proposed NSPU framework in terms of the tradeoff between model utility and unlearning efficacy, computational efficiency of the unlearning method, and privacy by measuring the separation quality score.

4.4. The Utility-Efficacy Tradeoff

GA and KLM cause catastrophic utility loss across LLM families. Both methods focus strictly on maximizing loss or divergence on forget data across LLM families. As detailed in Table 2, achieving higher harmonic perplexity values requires a higher forget gain and a lower retain cost. However, across the LLMs, the GA and KLM baselines exhibit both high forget gain and high retain cost. This indicates high uncertainty on both the forget and retain sets. While this reflects strong forgetting efficacy, it comes at the cost of severe utility degradation. The negative aggregate scores for GA and KLM underscore the nature of forget-loss approaches, which lack the fundamental mechanism to preserve useful knowledge beyond the forget set.

GD, DPO and NPO provide moderate improvements but remain limited. GD incorporates joint retention-forgetting objectives for better stability across these LLMs, while DPO and NPO suppresses undesired outputs but shows inconsistent behavior due to preference calibration sensitivity. Both DPO and NPO offer improved trade-offs over pure ascent techniques yet lack the robustness needed for scalable unlearning across diverse architectures.

NSPU consistently outperforms baseline unlearning methods. NSPU achieves positive and notably higher Aggregate scores across all tested models, while traditional approaches such as GA and KLM consistently yield highly negative Aggregate values. This indicates that NSPU effectively balances forgetting targeted data while maintaining model utility on retained data, unlike GA and KLM, which

Table 2. Evaluation of the Effectiveness of different unlearning methods in comparison with our approach on 5% forget set; Aggregate score is the cumulative sum of HCS+CES+HRS+HCNLL.

Model	Method	Perplexity			Truth Ratio			ROUGE-L			Probability			Aggregate
		G_F	C_R	HCS (\uparrow)	RS	FI	CES(\uparrow)	RR	FR	HRS (\uparrow)	G_{F_L}	C_{R_L}	HCNLL (\uparrow)	
Llama2-7B	GA	104.730	110.110	0.019	0.000	-0.805	-0.805	0.007	0.167	0.014	83.887	49.734	0.024	-0.748
	GD	4.597	6.006	0.420	0.497	0.054	0.551	0.210	0.245	0.399	4.811	3.988	0.395	1.765
	KLM	104.730	110.110	0.019	0.000	-0.808	-0.808	0.007	0.167	0.014	83.887	49.734	0.024	-0.751
	DPO	4.082	6.780	0.473	0.000	-0.998	-0.998	0.042	0.225	0.083	5.043	5.312	0.382	-0.060
	NPO	39.850	37.772	0.050	0.000	0.920	0.920	0.001	0.031	0.002	32.027	17.946	0.062	1.034
	NSPU	1.388	2.055	1.067	1.021	0.498	1.519	0.581	0.705	0.824	2.590	2.331	0.662	4.073
Mistral-7B	GA	154.695	202.520	0.013	0.000	-0.995	-0.995	0.034	0.112	0.068	124.738	74.003	0.016	-0.899
	GD	18.287	17.198	0.109	0.943	-0.511	0.432	0.363	0.375	0.639	1.258	1.551	1.051	2.232
	KLM	193.398	209.753	0.010	0.000	-1.001	-1.001	0.034	0.112	0.068	124.738	74.003	0.016	-0.907
	DPO	27.660	25.787	0.072	0.000	-0.554	-0.554	0.006	0.099	0.012	17.218	9.888	0.115	-0.355
	NPO	9.549	7.433	0.207	0.000	0.996	0.996	0.001	0.146	0.001	9.595	3.561	0.203	1.406
	NSPU	-0.084	2.066	4.995	0.921	-0.536	0.385	0.876	0.542	1.188	0.955	1.650	1.281	7.849
OLMoE	GA	84.662	87.404	0.024	0.000	-3.189	-3.189	0.006	0.068	0.012	65.839	71.628	0.030	-3.123
	GD	6.214	9.374	0.316	1.202	-1.924	-0.722	0.054	0.081	0.108	4.901	8.573	0.399	0.101
	KLM	84.662	87.404	0.024	0.000	-3.179	-3.179	0.006	0.077	0.012	65.839	71.628	0.030	-3.113
	DPO	1.887	-0.200	-0.645	0.000	-0.953	-0.953	0.705	0.560	1.011	1.929	0.831	0.638	0.051
	NPO	0.095	0.318	0.617	1.025	1.156	2.181	1.007	0.730	1.160	0.703	0.636	0.879	4.837
	NSPU	0.631	2.008	1.771	2.980	1.548	4.528	0.857	0.408	1.270	1.415	2.483	1.100	8.669
Llama-13B	GA	62.572	75.388	0.032	0.000	-0.362	-0.362	0.002	0.164	0.004	15.695	27.613	0.127	-0.199
	GD	0.067	0.077	0.154	0.598	0.762	1.360	0.765	1.454	0.724	1.329	0.977	0.850	3.088
	KLM	61.507	72.625	0.033	0.000	-1.002	-1.002	0.001	0.164	0.002	26.829	26.125	0.074	-0.893
	DPO	0.065	0.115	0.228	0.454	0.710	1.164	0.651	0.664	0.909	1.737	1.367	0.810	3.111
	NPO	6.958	11.820	0.284	0.472	1.115	0.356	0.747	0.345	1.188	2.020	3.213	0.858	2.686
	NSPU	1.173	1.445	1.072	0.987	0.736	1.723	0.817	0.518	1.148	1.480	1.535	0.938	4.882

aggressively forget but cause severe degradation in overall performance.

Takeaway 1: NSPU’s multi-metric aggregation, combining measures of uncertainty, veracity, and generative fidelity provides more nuanced control, avoiding extremes and yielding robust, effective unlearning.

Table 3. Computational costs (FLOPs) across methods for various LLMs

Methods	LLaMA-7B	Mistral-7B	OLMoE-1B-7B	LLaMA-13B
Retraining	8.40×10^{22}	3.36×10^{22}	3.00×10^{22}	8.40×10^{26}
GA	1.29×10^{17}	1.29×10^{16}	1.84×10^{16}	1.29×10^{21}
GD	5.16×10^{17}	5.16×10^{17}	7.37×10^{16}	5.16×10^{21}
KLM	1.29×10^{17}	1.29×10^{16}	1.84×10^{16}	1.29×10^{21}
DPO	5.16×10^{17}	5.16×10^{17}	7.37×10^{16}	5.16×10^{21}
NPO	5.16×10^{17}	5.16×10^{17}	7.37×10^{16}	5.16×10^{21}
NSPU	7.63×10^{16}	7.63×10^{15}	8.67×10^{15}	7.63×10^{20}

4.5. Computational efficiency analysis

To assess the computational efficiency of the NSPU method compared to baseline approaches, we compute the Floating point operations (FLOPs) required by each method. By following Brown et al. (2020); Yao et al. (2024a), we estimate the total training floating point operations (FLOPs) as $6 \times$ Total Training Tokens \times Parameter Size, and the total forward FLOPs as $2 \times$ Total Forward Tokens \times Parameter Size. As shown in Table 3, our approach requires 10 times fewer FLOPs than any baseline across the evaluated LLMs.

Further NSPU technique is 10^6 times more computationally efficient than retraining the model from scratch. Additionally, Appendix H.2 Figure 10 compares the VRAM consumption of various baseline unlearning methods with our proposed NSPU approach across different models. Since NSPU performs unlearning without any additional training, it requires significantly less computational resources compared to existing baselines.

Takeaway 2: NSPU $> 10^6 \times$ more computationally efficient than retraining, $10 \times$ vs. unlearning baselines.

4.6. Membership Inference and Separation Quality

Membership Inference Attacks (MIAs) evaluate unlearning efficacy by testing whether an adversary can distinguish forget set samples from unseen data using the unlearned model’s predictions (Shokri et al., 2017; Carlini et al., 2022; Maini et al., 2024b). Effective unlearning implies that the target model should perceive the forget set as indistinguishable from a non-member set (unseen data), while retaining performance on the retain set. To quantify this behavior, we construct the non-member set as detailed in Appendix K. To quantify MIA resistance, we compute mean Causal Language Modeling (CLM) loss across retain (M_R), forget (M_F), and non-member (M_{NM}) sets. The *Separation Quality Score* (SQS) measures how well the forget set loss aligns

Table 4. Separation quality score comparison for various unlearning methods, where forget loss distribution is compared against retain and non-member loss distributions, across various LLMs.

Method	Llama-7B	Mistral-7B	OLMoE-1B-7B	Llama-13B	Avg. (↑)
GA	0.798	0.785	0.765	0.403	0.688
GD	0.751	0.629	0.691	0.565	0.659
KLM	0.798	0.785	0.765	0.403	0.688
DPO	0.698	0.462	0.706	0.528	0.599
NPO	0.650	0.737	0.175	0.694	0.564
NSPU	0.833	0.794	0.742	0.723	0.773

with non-members while diverging from retain samples:

$$SQS = \frac{|M_R - M_F|}{|M_R - M_F| + |M_{NM} - M_F|} \quad (14)$$

The numerator maximizes forget-retain divergence (successful unlearning), while the denominator minimizes forget-nonmember divergence (MIA resistance). Higher SQS indicates stronger privacy preservation against membership inference. Table 4 reports SQS across models and domains.

Takeaway 3: High SQS scores reflects the balance between effective forgetting and retention, serving as a direct measure of privacy strength and unlearning fidelity.

5. Ablation studies

Beyond NSPU’s utility, efficiency, and privacy advantages, it is equally critical to assess its ability to precisely distinguish retain vs. forget information and to effectively identify domain-specific and entity-level (PII) knowledge. This perspective motivates deeper ablations on where and how unlearning occurs.

5.1. Interpretable View of Knowledge Separation

The final hidden layer is optimal for applying UL_{filter} . To determine the most effective layer for applying the UL_{filter} derived in Section 3.6, we analyze the layer-wise drift between the forget set and retain set activation vectors of the target model and its unlearned counterpart. The drift is quantified using (1) the centroid distance between the corresponding activation vectors in the original target model and (2) the maximum mean discrepancy (MMD) between these vectors (More details on Centroid distance and MMD in Appendix F). Both metrics exhibit a steady increase in separation across deeper layers, as illustrated in Figure 4. This trend indicates that the UL_{filter} effectively projects away task-specific information at the final layers, motivating its placement at the final hidden layer for maximum unlearning efficacy.

NSPU clearly distinguishes the forget and retain information. Figure 5 represents the distributional shift in the

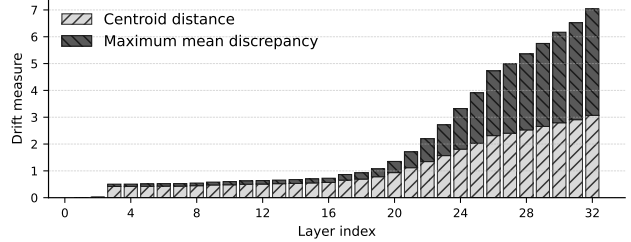


Figure 4. Layer-wise drift in activation vectors between target model (Mistral-7b-ins) and its unlearned version.

Table 5. Domain-wise similarity between the original (non-anonymized) activation vectors and the estimated activation vectors by the Latent representation aligner; DI - Digital informatics.

Domain	Llama-7B	Mistral-7B	OLMoE-1B-7B	Llama-13B
DI	0.64	0.49	0.63	0.82
Politics	0.80	0.70	0.76	0.87
Finance	0.79	0.70	0.74	0.87
Sports	0.76	0.60	0.70	0.84
Science	0.58	0.47	0.57	0.79
Average	0.71	0.59	0.68	0.84

activation vectors across layers: first, middle, and last of the original model and its unlearned counterpart. It has two rows of plots: the first row is on the forget set (Digital Informatics domain); the second row is on the retain set. The unlearning filter is incorporated at layer 31 of the model (Mistral-7B-Instruct-v0.1). Hence, the activation vectors of both the original and the unlearned models are identical until the 31st layer. In the 32nd layer (which is the last layer, including the initial embedding layer), we notice the impact of unlearning. The forget set is clearly separable by a large margin. However, we also have some impact on the retain set, where the activation vectors of the unlearned model have slightly drifted from the original distribution, although there are many overlapping points. Appendix Figure 18 proves a similar observation for Llama-13B, where the unlearning filter is applied at layer-39.

5.2. Identification of desired information to unlearn

NSPU effectively unlearns targeted domain information. To validate whether the proposed NSPU truly removes the intended information, rather than discarding unrelated or spurious knowledge, we conduct an ablation examining the nature of the “forgotten” content. Since the shadow unlearning process operates on anonymized data, it becomes essential to verify that the model is indeed forgetting the specific entity associated with each unlearning request. The Latent Representation Aligner plays a crucial role here—it bridges anonymized and original representations while maintaining inversion resistance to prevent sensitive information leakage. Although Appendix Table 9 demonstrates the overall performance of this deanonymization module, it is

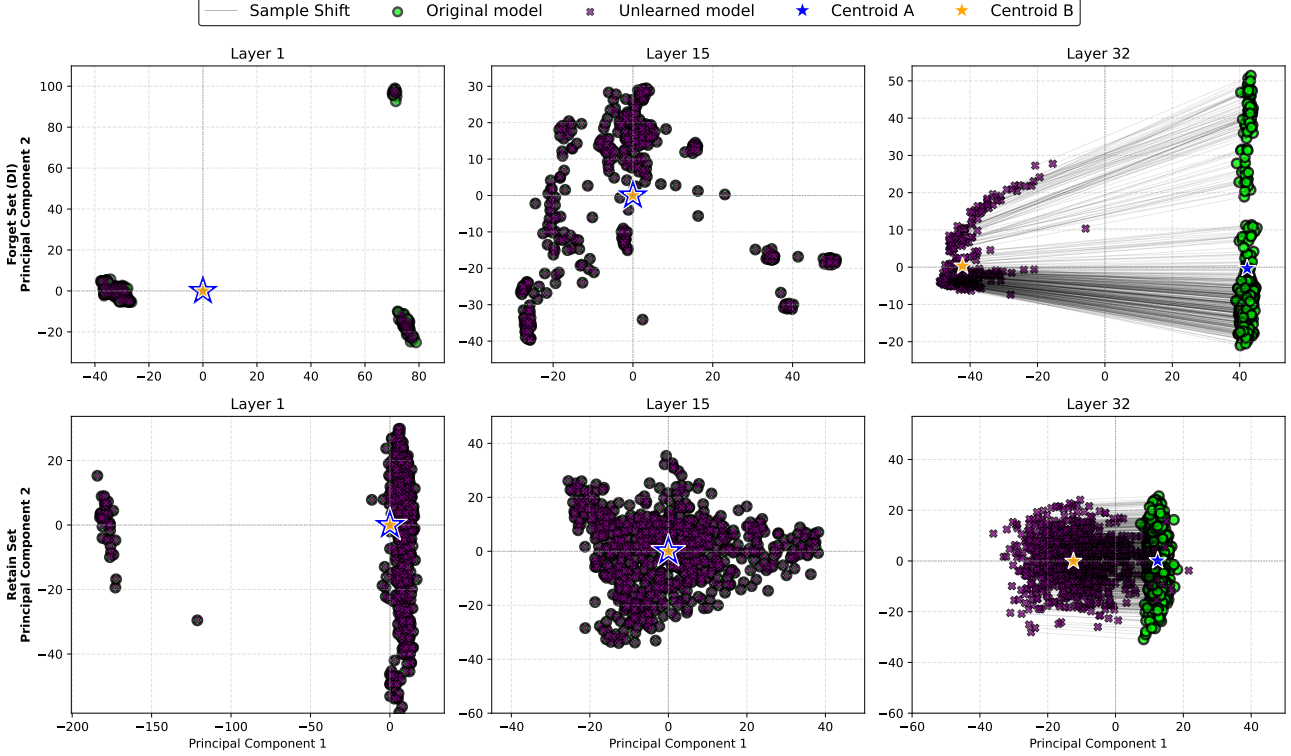


Figure 5. Impact of unlearning on forget and retain datasets before and after applying the unlearning filter (Mistral-7b-ins). Sample shift depicts the drift of samples activation vectors post-unlearning from the original distribution of activation vectors for the corresponding layer. **(Best viewed in color)**

Table 6. PII attribute-wise similarity score between the original (non-anonymized) activation vectors and estimated activation vectors by the Latent representation aligner in Single-entity samples of Sports domain (Model: Llama-13B)

PERSON	LOCATION	PHONE_NUMBER	DATE_TIME	Misc
0.85	0.84	0.84	0.80	0.83

equally important to assess how closely the reconstructed activation vectors approximate the original non-anonymized activations. Table 5 reports the domain-wise similarity between these pairs across different models. We incorporate an *InvOptScore* regularization term that penalizes overly high similarity, thereby balancing semantic alignment with privacy preservation. The obtained results show that the projected vectors maintain meaningful semantic correspondence to their originals, confirming the module’s ability to localize the correct knowledge while respecting data privacy constraints.

NSPU precisely removes the targeted entity information. To further investigate whether NSPU unlearns the correct information associated with each unlearning request, we perform a fine-grained, attribute-level analysis. This study isolates single-entity samples to eliminate potential confounding factors arising from co-occurring entities. Table

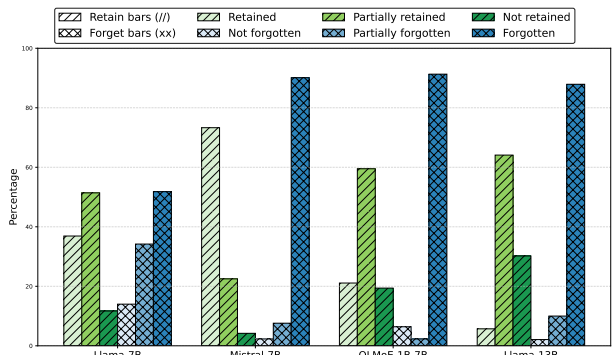


Figure 6. LLM-based evaluation results for the unlearned model on both forget and retain datasets.

6 presents the corresponding entity-wise cosine similarity scores. The results reinforce our hypothesis—NSPU consistently erases the intended entity representations, thereby satisfying the objective of faithful and entity-specific unlearning while retaining remaining domain knowledge.

5.3. LLM-based evaluation

We utilized the GPT-4o-mini (Achiam et al., 2023) model as an LLM-as-a-Judge to evaluate the quality of the outputs

generated by the unlearned model on both forget and retain datasets. The evaluation setup involved assessing whether the responses from each model were correct, partially correct, or incorrect, based on the samples from the retain and forget datasets. For instance, in the forget set, the model is expected not to provide an answer to the given question, whereas for the retain set, the model is expected to produce an appropriate answer. As depicted in Table 6, all the models demonstrate high retention percentages on the retain dataset, which signifies the robustness and effectiveness of the proposed NSPU method in preserving essential knowledge. Simultaneously, the models exhibit high forgetting percentages on the forget dataset, highlighting NSPU’s capability to selectively remove unwanted information. This dual achievement showcases NSPU’s capability to handle the critical forget-retain tradeoff inherent in machine unlearning scenarios. More details on the prompt used for the evaluation and reliability of the LLM-based evaluation details can be found in Appendix G.

5.4. Additional results

We provide more results and ablations, including: training of Latent representation aligner (Appendix B), human evaluation (Appendix G.1), computational efficiency analysis (Appendix H) based on FLOPS and VRAM, domain-specific performance evaluation (Appendix I), NSPU performance on downstream tasks (Appendix J), error analysis (Appendix L) and robustness evaluation of NSPU (Appendix M).

6. Conclusion

In this paper, we introduce shadow unlearning, a paradigm for privacy-preserving unlearning operates on an anonymized forget set, along with a specific unlearning method, Neuro-Semantic Projector Unlearning (NSPU). NSPU outperforms several unlearning baselines by achieving stronger knowledge retention and forgetting efficacy, as demonstrated through a comprehensive suite of evaluation metrics. It also offers computational efficiency, supported by a detailed FLOPs analysis, and ensures privacy protection, validated through membership-inference attacks and separation-quality assessments. Overall, our work opens up a new direction for privacy-aware machine unlearning that effectively balances data protection, model utility, and efficiency.

7. Limitations

The proposed NSPU approach is applicable only to open-source models, and its performance depends on the overlap between the data distributions of the forget and retain datasets. To design an efficient deanonymizer module, need

to find appropriate public data for MLP training. The results proposed in this work rely on a synthetic author profile test set.

8. Reproducibility Statement

To ensure reproducibility of our results, we have thoroughly documented all experimental details and evaluation procedures with proper grounding. All experiments were conducted using fixed random seeds to guarantee deterministic behavior across runs. We release our implementation code, detailed experimental scripts, and the dataset to facilitate the exact reproduction of our reported results.

9. Impact Statement

This work advances responsible and privacy-aware deployment of large language models through Shadow Unlearning. The proposed paradigm enables effective machine unlearning using anonymized forget data, reducing exposure of personally identifiable information during the unlearning process. By decoupling unlearning from direct access to sensitive data, our approach supports compliance with privacy regulations such as the GDPR’s Right to be Forgotten. It also resolves a critical privacy paradox present in existing unlearning methods.

References

Achiam, J., Adler, S., Agarwal, S., Ahmad, L., Akkaya, I., Aleman, F. L., Almeida, D., Altenschmidt, J., Altman, S., Anadkat, S., et al. Gpt-4 technical report. *arXiv preprint arXiv:2303.08774*, 2023.

Bhaila, K., Van, M.-H., and Wu, X. Soft prompting for unlearning in large language models. In *Proceedings of the 2025 Conference of the Nations of the Americas Chapter of the Association for Computational Linguistics: Human Language Technologies (Volume 1: Long Papers)*, pp. 4046–4056, 2025.

Bourtoule, L., Chandrasekaran, V., Choquette-Choo, C. A., Jia, H., Travers, A., Zhang, B., Lie, D., and Papernot, N. Machine unlearning. In *2021 IEEE symposium on security and privacy (SP)*, pp. 141–159. IEEE, 2021.

Brophy, J. and Lowd, D. Machine unlearning for random forests. In *International Conference on Machine Learning*, pp. 1092–1104. PMLR, 2021.

Brown, T., Mann, B., Ryder, N., Subbiah, M., Kaplan, J. D., Dhariwal, P., Neelakantan, A., Shyam, P., Sastry, G., Askell, A., et al. Language models are few-shot learners. *Advances in neural information processing systems*, 33: 1877–1901, 2020.

Cao, Y. and Yang, J. Towards making systems forget with machine unlearning. In *2015 IEEE symposium on security and privacy*, pp. 463–480. IEEE, 2015.

Carlini, N., Chien, S., Nasr, M., Song, S., Terzis, A., and Tramer, F. Membership inference attacks from first principles. In *2022 IEEE symposium on security and privacy (SP)*, pp. 1897–1914. IEEE, 2022.

Cha, S., Cho, S., Hwang, D., and Lee, M. Towards robust and parameter-efficient knowledge unlearning for llms. In *The Thirteenth International Conference on Learning Representations*, 2025.

Chen, M., Zhang, Z., Wang, T., Backes, M., Humbert, M., and Zhang, Y. When machine unlearning jeopardizes privacy. In *Proceedings of the 2021 ACM SIGSAC conference on computer and communications security*, pp. 896–911, 2021.

Choi, M., Rim, D., Lee, D., and Choo, J. Snap: Unlearning selective knowledge in large language models with negative instructions. *arXiv e-prints*, pp. arXiv-2406, 2024.

Chundawat, V. S., Tarun, A. K., Mandal, M., and Kankanhalli, M. Zero-shot machine unlearning. *IEEE Transactions on Information Forensics and Security*, 18:2345–2354, 2023.

Clark, P., Cowhey, I., Etzioni, O., Khot, T., Sabharwal, A., Schoenick, C., and Tafjord, O. Think you have solved question answering? try arc, the ai2 reasoning challenge. *arXiv preprint arXiv:1803.05457*, 2018.

Comanici, G., Bieber, E., Schaeckermann, M., Pasupat, I., Sachdeva, N., Dhillon, I., Blstein, M., Ram, O., Zhang, D., Rosen, E., et al. Gemini 2.5: Pushing the frontier with advanced reasoning, multimodality, long context, and next generation agentic capabilities. *arXiv preprint arXiv:2507.06261*, 2025.

Domingo-Ferrer, J., Jebreel, N., and Sánchez, D. Efficient unlearning with privacy guarantees. *arXiv preprint arXiv:2507.04771*, 2025.

Dou, G., Liu, Z., Lyu, Q., Ding, K., and Wong, E. Avoiding copyright infringement via large language model unlearning. In *Findings of the Association for Computational Linguistics: NAACL 2025*, pp. 5176–5200, 2025.

Eldan, R. and Russinovich, M. Who's harry potter? approximate unlearning in llms, 2023. URL <https://arxiv.org/abs/2310.02238>, 1(2):8.

Gao, C., Wang, L., Weng, C., Wang, X., and Zhu, Q. Practical unlearning for large language models. *arXiv preprint arXiv:2407.10223v1*, 2024a.

Gao, J., Garg, S., Mahmood, M., and Vasudevan, P. N. Deletion inference, reconstruction, and compliance in machine (un) learning. *Proceedings on Privacy Enhancing Technologies*, 2022(3), 2022.

Gao, X., Ma, X., Wang, J., Sun, Y., Li, B., Ji, S., Cheng, P., and Chen, J. Verifi: Towards verifiable federated unlearning. *IEEE Transactions on Dependable and Secure Computing*, 21(6):5720–5736, 2024b.

GDPR.eu. Article 17: Right to be forgotten, 2018a. URL <https://gdpr.eu/article-17-right-to-be-forgotten/>. [Accessed: 2025-11-14].

GDPR.eu. Recital 74: Responsibility and liability of the controller, 2018b. Available at: <https://gdpr.eu/recital-74-responsibility-and-liability-of-the-controller/> [Accessed: 2025-11-14].

Ginart, A., Guan, M., Valiant, G., and Zou, J. Y. Making ai forget you: Data deletion in machine learning. *Advances in neural information processing systems*, 32, 2019.

Golatkar, A., Achille, A., and Soatto, S. Eternal sunshine of the spotless net: Selective forgetting in deep networks. In *Proceedings of the IEEE/CVF conference on computer vision and pattern recognition*, pp. 9304–9312, 2020.

Gretton, A., Borgwardt, K. M., Rasch, M., Schölkopf, B., and Smola, A. J. A kernel two-sample test. *Journal of Machine Learning Research*, 13(Mar):723–773, 2012.

Gu, K., Rashid, M. R. U., Sultana, N., and Mehnaz, S. Second-order information matters: Revisiting machine unlearning for large language models. *arXiv preprint arXiv:2403.10557*, 2024.

Hendrycks, D., Burns, C., Basart, S., Zou, A., Mazeika, M., Song, D., and Steinhardt, J. Measuring massive multitask language understanding. In *International Conference on Learning Representations*, 2021.

Hu, H., Wang, S., Dong, T., and Xue, M. Learn what you want to unlearn: Unlearning inversion attacks against machine unlearning. In *2024 IEEE Symposium on Security and Privacy (SP)*, pp. 3257–3275. IEEE, 2024.

Huang, J. Y., Zhou, W., Wang, F., Morstatter, F., Zhang, S., Poon, H., and Chen, M. Offset unlearning for large language models. *Transactions on Machine Learning Research*.

Ishibashi, Y. and Shimodaira, H. Knowledge sanitization of large language models. *arXiv preprint arXiv:2309.11852*, 2023.

Izzo, Z., Smart, M. A., Chaudhuri, K., and Zou, J. Approximate data deletion from machine learning models. In *International conference on artificial intelligence and statistics*, pp. 2008–2016. PMLR, 2021.

Jang, J., Yoon, D., Yang, S., Cha, S., Lee, M., Logeswaran, L., and Seo, M. Knowledge unlearning for mitigating privacy risks in language models. In *Proceedings of the 61st Annual Meeting of the Association for Computational Linguistics (Volume 1: Long Papers)*, pp. 14389–14408, 2023.

Ji, J., Liu, Y., Zhang, Y., Liu, G., Kompella, R. R., Liu, S., and Chang, S. Reversing the forget-retain objectives: An efficient llm unlearning framework from logit difference. *Advances in Neural Information Processing Systems*, 37: 12581–12611, 2024.

Jia, J., Zhang, Y., Zhang, Y., Liu, J., Runwal, B., Diffenderfer, J., Kailkhura, B., and Liu, S. Soul: Unlocking the power of second-order optimization for llm unlearning. In *Proceedings of the 2024 Conference on Empirical Methods in Natural Language Processing*, pp. 4276–4292, 2024.

Jiang, A. Q., Sablayrolles, A., Mensch, A., Bamford, C., Chaplot, D. S., Casas, D. d. l., Bressand, F., Lengyel, G., Lample, G., Saulnier, L., et al. Mistral 7b. *arXiv preprint arXiv:2310.06825*, 2023.

Li, N., Pan, A., Gopal, A., Yue, S., Berrios, D., Gatti, A., Li, J. D., Dombrowski, A.-K., Goel, S., Mukobi, G., et al. The wmdp benchmark: Measuring and reducing malicious use with unlearning. In *International Conference on Machine Learning*, pp. 28525–28550. PMLR, 2024.

Li, N., Zhou, C., Gao, Y., Chen, H., Zhang, Z., Kuang, B., and Fu, A. Machine unlearning: Taxonomy, metrics, applications, challenges, and prospects. *IEEE Transactions on Neural Networks and Learning Systems*, 2025.

Lin, C.-Y. ROUGE: A package for automatic evaluation of summaries. In *Text Summarization Branches Out*, pp. 74–81, Barcelona, Spain, July 2004. Association for Computational Linguistics.

Lin, S., Hilton, J., and Evans, O. Truthfulqa: Measuring how models mimic human falsehoods. In *Proceedings of the 60th annual meeting of the association for computational linguistics (volume 1: long papers)*, pp. 3214–3252, 2022.

Liu, B., Liu, Q., and Stone, P. Continual learning and private unlearning. In *Conference on Lifelong Learning Agents*, pp. 243–254. PMLR, 2022a.

Liu, C., Wang, Y., Flanigan, J., and Liu, Y. Large language model unlearning via embedding-corrupted prompts. *Advances in Neural Information Processing Systems*, 37: 118198–118266, 2024a.

Liu, Y., Chen, H., Huang, W., Ni, Y., and Imani, M. Lune: Efficient llm unlearning via lora fine-tuning with negative examples. In *Socially Responsible and Trustworthy Foundation Models at NeurIPS 2025*.

Liu, Y., Xu, L., Yuan, X., Wang, C., and Li, B. The right to be forgotten in federated learning: An efficient realization with rapid retraining. In *IEEE INFOCOM 2022-IEEE conference on computer communications*, pp. 1749–1758. IEEE, 2022b.

Liu, Z., Dou, G., Chien, E., Zhang, C., Tian, Y., and Zhu, Z. Breaking the trilemma of privacy, utility, and efficiency via controllable machine unlearning. In *Proceedings of the ACM Web Conference 2024*, pp. 1260–1271, 2024b.

Liu, Z., Dou, G., Tan, Z., Tian, Y., and Jiang, M. Towards safer large language models through machine unlearning. In *Findings of the Association for Computational Linguistics ACL 2024*, pp. 1817–1829, 2024c.

Liu, Z., Jiang, Y., Shen, J., Peng, M., Lam, K.-Y., Yuan, X., and Liu, X. A survey on federated unlearning: Challenges, methods, and future directions. *ACM Computing Surveys*, 57(1):1–38, 2024d.

Liu, Z., Ye, H., Chen, C., Zheng, Y., and Lam, K.-Y. Threats, attacks, and defenses in machine unlearning: A survey. *IEEE Open Journal of the Computer Society*, 2025.

Lu, W., Zeng, Z., Wang, J., Lu, Z., Chen, Z., Zhuang, H., and Chen, C. Eraser: Jailbreaking defense in large language models via unlearning harmful knowledge. *arXiv preprint arXiv:2404.05880*, 2024.

Maini, P., Feng, Z., Schwarzschild, A., Lipton, Z. C., and Kolter, J. Z. Tofu: A task of fictitious unlearning for llms. In *First Conference on Language Modeling*, 2024a.

Maini, P., Jia, H., Papernot, N., and Dziedzic, A. Llm dataset inference: Did you train on my dataset? *Advances in Neural Information Processing Systems*, 37:124069–124092, 2024b.

Mishra, K., Pagare, H., and Sharma, K. A hybrid rule-based nlp and machine learning approach for pii detection and anonymization in financial documents. *Scientific Reports*, 15(1):22729, 2025.

Muennighoff, N., Soldaini, L., Groeneveld, D., Lo, K., Morrison, J., Min, S., Shi, W., Walsh, E. P., Tafjord, O., Lambert, N., et al. Olmoe: Open mixture-of-experts language models. In *The Thirteenth International Conference on Learning Representations*.

Muresanu, A. I., Thudi, A., Zhang, M. R., and Papernot, N. Fast exact unlearning for in-context learning data for llms. In *Forty-second International Conference on Machine Learning*, 2025.

Nguyen, T. T., Huynh, T. T., Ren, Z., Nguyen, P. L., Liew, A. W.-C., Yin, H., and Nguyen, Q. V. H. A survey of machine unlearning. *ACM Transactions on Intelligent Systems and Technology*, 16(5):1–46, 2025.

Nicolazzo, S., Nocera, A., et al. How secure is forgetting? linking machine unlearning to machine learning attacks. *arXiv preprint arXiv:2503.20257*, 2025.

Pawelczyk, M., Neel, S., and Lakkaraju, H. In-context unlearning: Language models as few-shot unlearners. In *International Conference on Machine Learning*, pp. 40034–40050. PMLR, 2024.

Qu, Y., Yuan, X., Ding, M., Ni, W., Rakotoarivelo, T., and Smith, D. Learn to unlearn: Insights into machine unlearning. *Computer*, 57(3):79–90, 2024.

Rafailov, R., Sharma, A., Mitchell, E., Manning, C. D., Ermon, S., and Finn, C. Direct preference optimization: Your language model is secretly a reward model. *Advances in neural information processing systems*, 36: 53728–53741, 2023.

Schelter, S., Grafberger, S., and Dunning, T. Hedgecut: Maintaining randomised trees for low-latency machine unlearning. In *Proceedings of the 2021 International Conference on Management of Data*, pp. 1545–1557, 2021.

Shokri, R., Stronati, M., Song, C., and Shmatikov, V. Membership inference attacks against machine learning models. In *2017 IEEE symposium on security and privacy (SP)*, pp. 3–18. IEEE, 2017.

Su, N. and Li, B. Asynchronous federated unlearning. In *IEEE INFOCOM 2023-IEEE conference on computer communications*, pp. 1–10. IEEE, 2023.

Tang, H., Liu, Y., Zhao, X., Liu, X., Zhang, Y., Zhang, K., Zhou, X., and Chen, E. Learn while unlearn: An iterative unlearning framework for generative language models. *arXiv preprint arXiv:2407.20271*, 2024.

Thudi, A., Deza, G., Chandrasekaran, V., and Papernot, N. Unrolling sgd: Understanding factors influencing machine unlearning. In *2022 IEEE 7th European Symposium on Security and Privacy (EuroS&P)*, pp. 303–319. IEEE, 2022a.

Thudi, A., Jia, H., Shumailov, I., and Papernot, N. On the necessity of auditable algorithmic definitions for machine unlearning. In *31st USENIX security symposium (USENIX Security 22)*, pp. 4007–4022, 2022b.

Tian, B., Liang, X., Cheng, S., Liu, Q., Wang, M., Sui, D., Chen, X., Chen, H., and Zhang, N. To forget or not? towards practical knowledge unlearning for large language models. In *Findings of the Association for Computational Linguistics: EMNLP 2024*, pp. 1524–1537, 2024.

Touvron, H., Lavril, T., Izacard, G., Martinet, X., Lachaux, M.-A., Lacroix, T., Rozière, B., Goyal, N., Hambro, E., Azhar, F., et al. Llama: Open and efficient foundation language models. *arXiv preprint arXiv:2302.13971*, 2023a.

Touvron, H., Martin, L., Stone, K., Albert, P., Almahairi, A., Babaei, Y., Bashlykov, N., Batra, S., Bhargava, P., Bhosale, S., et al. Llama 2: Open foundation and fine-tuned chat models. *arXiv preprint arXiv:2307.09288*, 2023b.

Wang, B., Zi, Y., Sun, Y., Zhao, Y., and Qin, B. Balancing forget quality and model utility: A reverse kl-divergence knowledge distillation approach for better unlearning in llms. In *Proceedings of the 2025 Conference of the Nations of the Americas Chapter of the Association for Computational Linguistics: Human Language Technologies (Volume 1: Long Papers)*, pp. 1306–1321, 2025a.

Wang, F., Li, B., and Li, B. Federated unlearning and its privacy threats. *IEEE Network*, 38(2):294–300, 2024.

Wang, L., Zeng, X., Guo, J., Wong, K.-F., and Gottlob, G. Selective forgetting: Advancing machine unlearning techniques and evaluation in language models. In *Proceedings of the AAAI Conference on Artificial Intelligence*, volume 39, pp. 843–851, 2025b.

Wang, W., Tian, Z., Zhang, C., Liu, A., and Yu, S. Bfu: Bayesian federated unlearning with parameter self-sharing. In *Proceedings of the 2023 ACM Asia Conference on Computer and Communications Security*, pp. 567–578, 2023.

Wang, W., Tian, Z., Zhang, C., and Yu, S. Oblivious unlearning by learning: Machine unlearning without exposing erased data. 2025c.

Xu, J., Wu, Z., Wang, C., and Jia, X. Machine unlearning: Solutions and challenges. *IEEE Transactions on Emerging Topics in Computational Intelligence*, 8(3): 2150–2168, 2024.

Yao, J., Chien, E., Du, M., Niu, X., Wang, T., Cheng, Z., and Yue, X. Machine unlearning of pre-trained large language models. In Ku, L.-W., Martins, A., and Srikumar, V. (eds.), *Proceedings of the 62nd Annual Meeting of the Association for Computational Linguistics (Volume 1: Long Papers)*, pp. 8403–8419, Bangkok, Thailand, August 2024a. Association for Computational Linguistics. doi: 10.18653/v1/2024.acl-long.457.

Yao, Y., Xu, X., and Liu, Y. Large language model unlearning. *Advances in Neural Information Processing Systems*, 37:105425–105475, 2024b.

Yuan, X., Pang, T., Du, C., Chen, K., Zhang, W., and Lin, M. A closer look at machine unlearning for large language models. In *The Thirteenth International Conference on Learning Representations*, 2025.

Zhang, K., Wang, W., Fan, Z., Song, X., and Yu, S. Conditional matching gan guided reconstruction attack in machine unlearning. In *GLOBECOM 2023-2023 IEEE Global Communications Conference*, pp. 44–49. IEEE, 2023.

Zhang, R., Lin, L., Bai, Y., and Mei, S. Negative preference optimization: From catastrophic collapse to effective unlearning. In *First Conference on Language Modeling*, 2024.

Zhou, S., Wang, L., Ye, J., Wu, Y., and Chang, H. On the limitations and prospects of machine unlearning for generative ai. *arXiv preprint arXiv:2408.00376*, 2024.

Appendix

A. Synthetic Dataset Creation

To overcome the high degree of overlap between the retain and forget samples in the existing benchmark datasets, we create a TOFU-style synthetic dataset for the five different domains: Digital Informatics, Science and Technology, Sports, Finance, and Politics. We depict the overlap present in the TOFU forget and retain samples in Figure 7, TOFU retain, and our forget data samples t-sne plot presented in Table 8. Figure 9 further illustrates the overlap of various domains in our dataset.

Below is the prompt utilized to obtain the synthetic dataset using Gemini-2.5-Pro.

System Prompt for Synthetic Dataset Generation

The task is to generate a synthetic dataset to complement the existing TOFU Authors dataset while ensuring a distinguishable distribution shift. The original dataset follows a narrative biographical structure involving identity establishment, professional background, and work analysis. Your goal is to retain comparable data complexity while introducing new question–answer patterns that significantly deviate in structure and content.

Please adhere to the following requirements for dataset generation:

- **Volume:** Create 20 distinct sets of data. Each set must contain exactly 20 question-answer pairs, for a total of 400 pairs.
- **Core Content:** Every question-answer pair must involve a subject entity associated with some form of personally identifiable information (PII).
- **Answer Conciseness:** All answers must be concise and not exceed a maximum length of 20 words.
- **Distributional Drift:** The primary objective is to achieve the maximum possible distributional drift from the original dataset. The resulting samples should be reliably separable from the original dataset by a classifier.
- **Structural Variety:** Ensure internal variety by diversifying sentence structures and the contexts of entity–PII relationships (e.g., contact details, addresses, specific identifiers, etc.).

Critical Exclusions – Do NOT replicate the following patterns:

- **Narrative Structure:** Avoid any question-answer formation that replicates the narrative style of the original dataset. This includes:
 - Establishing identity (e.g., early life, origin, family).
 - Defining profession, listing awards, or detailing notable works.
 - Linking personal background to professional style or themes.
 - Analyzing fictional works.
 - Expanding a persona with biography-style details.
- **Topic-Based Exclusions:** Do not include aspects such as early life, bibliographic details, awards, achievements, motivations, or notable works.

B. Training of Latent Representation Aligner

B.1. Public data collection

The unknown and potentially multi-domain nature of the anonymized data necessitates the Latent representation aligner to be trained on heterogeneous data. For this purpose, we have combined six different PII datasets from different categories and formats, as depicted in 10. The curated training dataset for the projector consist of 21.24k (*original_text, anonymized_counterpart*) samples.

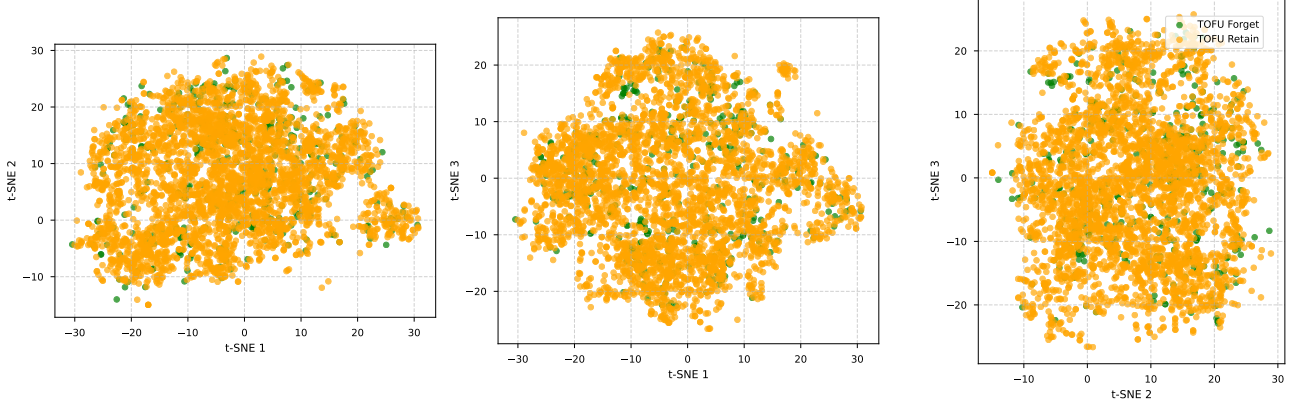


Figure 7. T-sne plot of activation vectors distribution of original forget and retain TOFU dataset

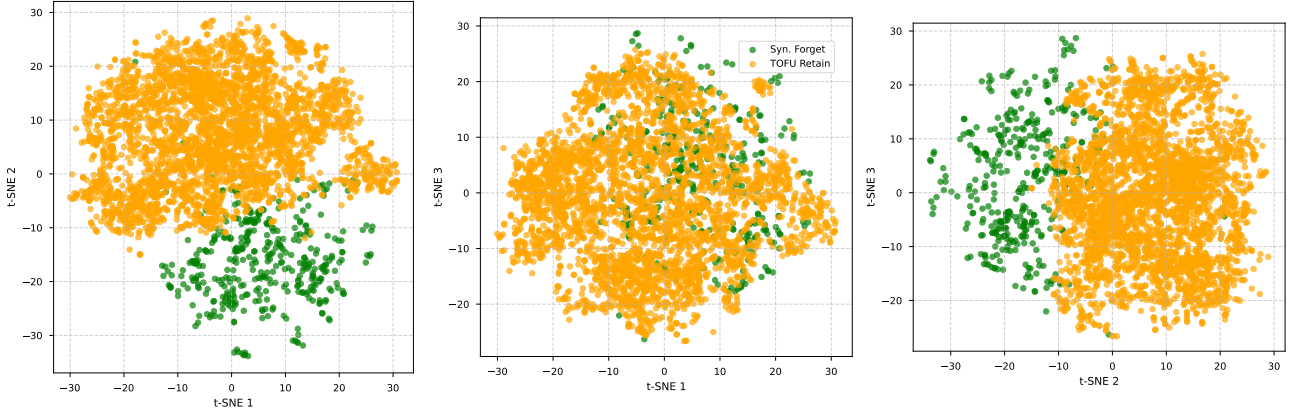


Figure 8. T-sne plot of activation vectors distribution of TOFU retain set and synthetic forget set

B.2. Training the MLP

To assess the recoverability of semantic information removed during anonymization, we train a lightweight Multilayer Perceptron (MLP) model designed to reconstruct the embedding of the original text from the embedding of its anonymized counterpart. The MLP is optimized using the mean squared error (MSE) objective. All experiments follow a standardized train-validation-test split. By posing reconstruction as a purely geometric mapping problem in the latent space, we obtain a model-agnostic probe for evaluating whether anonymized representations still encode residual semantic information about the original content.

Given an anonymized embedding \mathbf{x}_i and its corresponding original embedding \mathbf{y}_i , the reconstruction model learns a function f_θ parameterized by θ such that

$$\hat{\mathbf{y}}_i = f_\theta(\mathbf{x}_i), \quad (15)$$

where $\hat{\mathbf{y}}_i$ denotes the reconstructed embedding. The model is optimized using the Mean Squared Error (MSE) objective defined as

$$\mathcal{L}_{\text{MSE}} = \frac{1}{N} \sum_{i=1}^N \|\mathbf{y}_i - \hat{\mathbf{y}}_i\|_2^2, \quad (16)$$

where N is the number of training samples. Minimizing this loss encourages the network to produce reconstructed embeddings that closely approximate the original semantic representations.

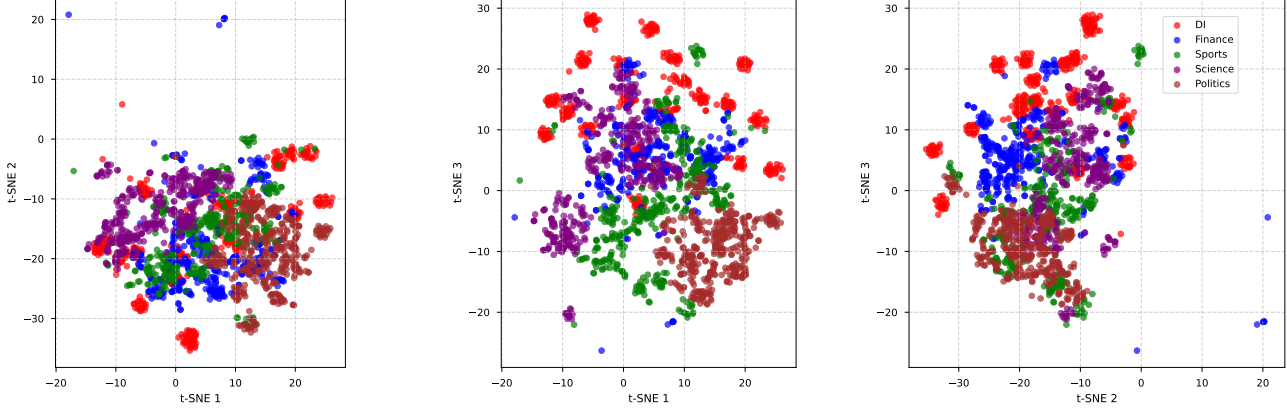


Figure 9. T-sne plot of activation vectors distribution of synthetic multi-domain forget sets

To assess the quality of reconstructing the original embedding \mathbf{y}_i from its anonymized counterpart, we compute a set of complementary evaluation metrics.

1. **Mean Squared Error (MSE).** The Mean Squared Error measures the average squared deviation between the true and reconstructed embeddings:

$$\text{MSE} = \frac{1}{N} \sum_{i=1}^N \|\mathbf{y}_i - \hat{\mathbf{y}}_i\|_2^2. \quad (17)$$

2. **Mean Absolute Error (MAE).** MAE quantifies the average magnitude of reconstruction error:

$$\text{MAE} = \frac{1}{N} \sum_{i=1}^N |\mathbf{y}_i - \hat{\mathbf{y}}_i|. \quad (18)$$

3. **Coefficient of Determination (R^2).** The R^2 metric measures the proportion of variance in the original embeddings explained by the reconstructed embeddings:

$$R^2 = 1 - \frac{\sum_{i=1}^N \|\mathbf{y}_i - \hat{\mathbf{y}}_i\|_2^2}{\sum_{i=1}^N \|\mathbf{y}_i - \bar{\mathbf{y}}\|_2^2}, \quad (19)$$

where $\bar{\mathbf{y}}$ denotes the mean embedding over the dataset.

Table 7. Domain-wise PII Distribution

PII Type	Sports	Finance	Digital Informatics	Science	Politics
PERSON	387	400	387	379	400
LOCATION	51	19	51	48	24
PHONE_NUMBER	40	7	40	0	49
EMAIL	20	0	20	0	25
DATE_TIME	33	49	33	100	18
IN_PAN	29	54	29	93	45
URL	8	22	8	12	12
US_DRIVER_LICENSE	17	5	17	49	147
NRP	17	3	17	1	2
Misc	49	28	49	1	36
Single-Entity	213	245	213	169	106
Multi-Entity	185	155	185	221	294
Total	400	400	400	400	400

Table 8. Aggregate PII Distribution

PII Type	Count
PERSON	1953
LOCATION	193
PHONE_NUMBER	136
EMAIL	65
DATE_TIME	233
IN_PAN	250
URL	62
US_DRIVER_LICENSE	235
NRP	40
Misc	76
Single-Entity	946
Multi-Entity	1040
Total	2000

Table 9. The MLP performance of various models across the overlap percentages; MSE - Mean Squared Error, MAE - Mean Absolute Error.

Model	% overlap	MSE	MAE	R ²	Cosine Sim.	Pearson Corr.
LLaMA-7B	5	0.086	0.222	0.671	0.926	0.926
	25	0.083	0.210	0.771	0.968	0.968
	50	0.068	0.186	0.751	0.956	0.956
	75	0.069	0.186	0.754	0.957	0.957
Mistral-7B Instruct	5	1.044	0.772	0.443	0.928	0.928
	25	1.040	0.769	-1.057	0.924	0.924
	50	1.089	0.784	-2.053	0.922	0.922
	75	1.116	0.794	0.263	0.923	0.923
OLMoE-1B-7B	5	1.044	0.772	0.443	0.928	0.928
	25	1.040	0.769	-1.057	0.924	0.924
	50	1.089	0.784	-2.053	0.922	0.922
	75	1.116	0.794	0.263	0.923	0.923
LLaMA-13B	5	0.026	0.120	0.566	0.945	0.945
	25	0.026	0.119	0.465	0.945	0.945
	50	0.026	0.120	0.573	0.945	0.945
	75	0.026	0.120	0.500	0.945	0.945

Table 10. Public data used for training Latent representation aligner

Dataset	PII Category	Trainset Samples	Samples used
Synthetic PII Finance	Finance	24158	5000
PII for Privacy	Health	135621	5000
Australian PII Dataset	Customer interaction	1240	1240
Implicit PII Detection	Synthetic profiles	5000	5000
NinjaMasker PII Redaction	Chat assistant	34700	5000
PII Masking-400k	General PII	326000	5000

4. **Cosine Similarity.** To measure semantic alignment, we compute cosine similarity between each original and reconstructed embedding:

$$\cos(\theta_i) = \frac{\mathbf{y}_i \cdot \hat{\mathbf{y}}_i}{\|\mathbf{y}_i\|_2 \|\hat{\mathbf{y}}_i\|_2}. \quad (20)$$

5. **Pearson Correlation.** Pearson correlation captures linear correlation between the embedding dimensions of \mathbf{y}_i and $\hat{\mathbf{y}}_i$:

$$\rho_i = \frac{\text{Cov}(\mathbf{y}_i, \hat{\mathbf{y}}_i)}{\sigma_{\mathbf{y}_i} \sigma_{\hat{\mathbf{y}}_i}}. \quad (21)$$

Table 11. Models used in our experiments.

Model name	Parameters count	Model type
Llama-7B	7B	Base
Mistral-7B-Instruct-v0.1	7B	Instruct
Llama-13B-Chat	13B	Chat
OLMoE-1B-7B-0924	1B (Active)	Mixture of Experts

Together, these metrics characterize both numerical fidelity (MSE, MAE), variance explanation (R^2), and structural or semantic similarity (cosine similarity and Pearson correlation). The performance of the evaluation metrics for various LLMs are detailed in Table 9.

C. Theoretical Guarantee for Forget Space Creation

As represented in Figure 3, the proposed methodology first implicitly decomposes v_{in} into its ‘forget’ component:

$$v_{in}^u = (UU^T)v_{in} \quad (22)$$

and its ‘safe’ component:

$$v_{in}^{u\perp} = (I - UU^T)v_{in} \quad (23)$$

Thus:

$$v_{in} = v_{in}^u + v_{in}^{u\perp} \quad (24)$$

It then subtracts a fraction of v_{in}^u from the original vector. The result:

$$v_{out} = v_{in} - \alpha v_{in}^u \quad (25)$$

is a vector steered away from the forget subspace. This attenuates information aligned with the concepts to be forgotten, while the safe component $v_{in}^{u\perp}$ is preserved intact.

α governs the strength or effectiveness of unlearning. When set to 1, v_{out} becomes $v_{in}^{u\perp}$, with no component along the forget subspace, thus, nullifying the entire forget set information from the model. However, this dents the semantic understanding and other general capabilities of the model. Therefore, α plays a crucial role to in deciding extent of unlearning with a tradeoff against the knowledge retention and multi-purpose general capabilities of the model.

Substituting equation (24) in equation (25):

$$v_{out} = v_{in}^{u\perp} + (1 - \alpha)v_{in}^u \quad (26)$$

$$v_{out} = v_{in} - v_{in}UU^T + (1 - \alpha)v_{in}UU^T \quad (27)$$

$$v_{out} = v_{in} - v_{in}UU^T + v_{in}UU^T - \alpha v_{in}UU^T \quad (28)$$

$$v_{out} = v_{in} - \alpha v_{in}UU^T \quad (29)$$

$$v_{out} = (I - \alpha v_{in}UU^T)v_{in} \quad (30)$$

Considering $(1 - \alpha v_{in}UU^T)$ as the UL_{filter} :

$$UL_{filter} = (I - \alpha v_{in}UU^T) \quad (31)$$

We get the final active unlearning equation as:

$$v_{out} = UL_{filter}v_{in} \quad (32)$$

D. Experimental Setup

We conduct all experiments using two Nvidia GeForce RTX A6000 (48GB) GPUs. Table 11 details the models used for our experiments, all of which were loaded in bfloat16 precision. We fine-tuned all models using a learning rate of 2e-5, a batch size of 8, and a maximum sequence length of 512. All other QLoRA² and Hugging Face Trainer³ parameters were kept to their default values. To obtain deterministic response generation and inference, ‘temperature’ was set to 0.001 and, sampling is disabled (*do_sample=False*) in all experiments. The hyperparameter values of α , the strength of UL_{filter} are presented in Table 12.

Table 12. The strength of Unlearning filter (α) of various models across the data overlap variants

Data overlap variant	Llama-7B	Mistral-7B	OLMoE-1B-7B	Llama-13B
5%	0.0103	0.01	0.085	0.0115
25%	0.0353	0.315	0.087	0.0097
50%	0.0380	0.01	0.08	0.029
75%	0.0405	0.115	0.08	0.0325

Choice of PCA Rank (k): Instead of defining a static PCA rank k of the forget subspace a priori, we employ an adaptive rank selection strategy based on explained variance. We perform PCA on the collected vectors and examine the cumulative explained variance ratio. We select the minimum number of components k required to account for 95% of the total variance ($\tau = 0.95$) in the data. Thus, k is chosen such that:

$$k = \min \left\{ d \in \mathbb{Z}^+ \mid \sum_{i=1}^d \lambda_i \geq 0.95 \sum_{j=1}^D \lambda_j \right\} \quad (33)$$

where λ_i represents the eigenvalue, which corresponds to the explained variance associated with the i^{th} principal component, and D is the original dimensionality of the vectors. This ensures that the subspace captures the dominant directions of the representation while discarding the bottom 5% as stochastic noise.

E. Formulations for Baseline Methods

We list the baseline unlearning algorithms provided in the TOFU (Maini et al., 2024a) benchmark, including Gradient Ascent (GA), Gradient Difference (GD), KL Minimization (KLM), Direct Preference Optimization (DPO), and Negative Preference Optimization (NPO).

Gradient Ascent (GA) (Thudi et al., 2022a) This method directly attempts to make the model “forget” target data by performing gradient ascent on the standard training loss with respect to the forget set \mathcal{D}_F . This is equivalent to minimizing the negative log-likelihood of the forget data. The unlearning objective $\mathcal{J}_{GA}(\theta)$ to be minimized is:

$$\mathcal{J}_{GA}(\theta) = -\mathcal{L}_{\mathcal{D}_F}(\theta) = -\frac{1}{|\mathcal{D}_F|} \sum_{d_f \in \mathcal{D}_F} \mathcal{L}(d_f; \theta)$$

where θ are the model parameters and $\mathcal{L}(d; \theta)$ is the loss for a single sample d .

Gradient Difference (GD) (Liu et al., 2022a) This approach extends GA by adding a competing objective: preserving model performance on the retain set \mathcal{D}_R . The objective function is formulated to simultaneously maximize the loss on \mathcal{D}_F (by minimizing its negative) and minimize the loss on \mathcal{D}_R . The combined objective $\mathcal{J}_{GD}(\theta)$ to be minimized is:

$$\mathcal{J}_{GD}(\theta) = \mathcal{L}_{\mathcal{D}_R}(\theta) - \lambda \cdot \mathcal{L}_{\mathcal{D}_F}(\theta)$$

where λ is a hyperparameter balancing the two objectives. During training, samples are drawn from both \mathcal{D}_R and \mathcal{D}_F to compute a stochastic gradient.

KL Minimization (KLM) (Chundawat et al., 2023) This method regularizes the unlearning process to prevent the model from deviating significantly from its original, general-purpose behavior. It combines the GA objective on \mathcal{D}_F with a

²<https://github.com/artidoro/qlora>

³https://huggingface.co/docs/transformers/main_classes/trainer

regularization term that minimizes the Kullback-Leibler (KL) divergence between the output distributions of the original reference model, π_{ref} , and the current unlearning model, π_{θ} , on the retain set \mathcal{D}_R . The objective $\mathcal{J}_{KL}(\theta)$ to be minimized is:

$$\mathcal{J}_{KL}(\theta) = -\mathcal{L}_{\mathcal{D}_F} l(\theta) + \beta \cdot \mathbb{E}_{s \in \mathcal{D}_R} [D_{KL}(\pi_{\text{ref}}(\cdot|s) \parallel \pi_{\theta}(\cdot|s))]$$

where β is a weighting coefficient.

Direct Preference Optimization (DPO) (Rafailov et al., 2023) formulates alignment as a pairwise preference learning problem, in which the model is trained to prefer a desirable response over an undesirable one for a given prompt.

Given a prompt x , a preferred response y_w , and a dispreferred response y_l , the DPO objective directly optimizes the policy π_{θ} without explicit reward modeling. The loss is defined as:

$$\mathcal{L}_{\text{DPO},\beta}(\theta) = -\mathbb{E}_{(x,y_w,y_l) \sim \mathcal{D}} \left[\log \sigma \left(\beta \log \frac{\pi_{\theta}(y_w|x)}{\pi_{\text{ref}}(y_w|x)} - \beta \log \frac{\pi_{\theta}(y_l|x)}{\pi_{\text{ref}}(y_l|x)} \right) \right]$$

where π_{ref} is a fixed reference model and β controls the sharpness of preference enforcement. This objective encourages the policy to increase the relative likelihood of preferred responses over dispreferred ones. We have leveraged the dispreferred responses from (Maini et al., 2024a).

Negative Preference Optimization (NPO) (Zhang et al., 2024) formulates unlearning as the direct suppression of undesired responses, without requiring the specification of a preferred alternative.

Unlearning can be formulated as a special case of preference optimization in which only negative (forgotten) responses are available. Specifically, for each $(x, y) \in \mathcal{D}_F$, the response y is treated as a dispreferred output with no corresponding positive alternative. By removing the positive term from the DPO objective, the NPO loss is obtained as:

$$\mathcal{L}_{\text{NPO},\beta}(\theta) = -\frac{2}{\beta} \mathbb{E}_{(x,y) \sim \mathcal{D}_F} \left[\log \sigma \left(-\beta \log \frac{\pi_{\theta}(y|x)}{\pi_{\text{ref}}(y|x)} \right) \right]$$

Minimizing this objective suppresses the relative likelihood of forgotten outputs under π_{θ} while maintaining stability via the reference model.

F. Quantifying Layer-wise Drift in Activation Vectors

To quantify the layer-wise representational drift induced by the unlearning process, we analyze the divergence between the activation vectors of the target model M_{target} and the unlearned model M_{unlearn} . Let $\mathcal{X} = \{x_1, \dots, x_N\}$ denote the forget dataset. For a given layer l , let $A^{(l)} = \{h^{(l)}(x) \mid x \in \mathcal{X}\} \subset \mathbb{R}^{d_l}$ represent the set of activation vectors from the target model, and $\tilde{A}^{(l)} = \{\tilde{h}^{(l)}(x) \mid x \in \mathcal{X}\} \subset \mathbb{R}^{d_l}$ represent the corresponding activations from the unlearned model.

F.1. Centroid Distance

The Centroid distance measures the magnitude of the shift in the mean activation vector at layer l . Rather than measuring individual sample perturbations, this metric captures the global displacement of the feature cluster's geometric centroid. We define the layer-wise centroids $\mu^{(l)}$ and $\tilde{\mu}^{(l)}$ as:

$$\mu^{(l)} = \frac{1}{N} \sum_{i=1}^N h^{(l)}(x_i), \quad \tilde{\mu}^{(l)} = \frac{1}{N} \sum_{i=1}^N \tilde{h}^{(l)}(x_i) \tag{34}$$

The Centroid distance is formally defined as the L_2 norm of the difference between these centroids:

$$D_{\text{Centroid}}(A^{(l)}, \tilde{A}^{(l)}) = \|\mu^{(l)} - \tilde{\mu}^{(l)}\|_2 \tag{35}$$

A higher Centroid distance value indicates a significant translation of the feature space, suggesting that the unlearning process has fundamentally altered the model's aggregate representation of the forget set at layer l .

F.2. Maximum Mean Discrepancy (MMD)

While Centroid distance captures the first-order shift, it might not be sufficient for detecting changes in the distributional geometry. To assess the comprehensive distributional divergence between $A^{(l)}$ and $\tilde{A}^{(l)}$, we employ the Maximum Mean Discrepancy (MMD) (Gretton et al., 2012). MMD is a kernel-based statistical test that maps the activation distributions into a Reproducing Kernel Hilbert Space (RKHS) \mathcal{H} to compare their higher-order moments.

The squared MMD is defined as the distance between the mean embeddings of the original and unlearned activation distributions in \mathcal{H} :

$$\text{MMD}^2(A^{(l)}, \tilde{A}^{(l)}) = \left\| \frac{1}{N} \sum_{i=1}^N \phi(h_i^{(l)}) - \frac{1}{N} \sum_{j=1}^N \phi(\tilde{h}_j^{(l)}) \right\|_{\mathcal{H}}^2 \quad (36)$$

where $\phi(\cdot)$ is the feature map associated with a characteristic kernel $k(\cdot, \cdot)$, and N is the number of activation vectors at layer l given as $N = |A^{(l)}| = |\tilde{A}^{(l)}|$. In our experiments, we compute an empirical estimate of MMD^2 using the Gaussian Radial Basis Function (RBF) kernel $k(x, y) = \exp(-\frac{\|x-y\|^2}{2\sigma^2})$, implemented via standard pairwise kernel evaluations. The biased empirical estimator is computed as:

$$\widehat{\text{MMD}}_{\text{biased}}^2 = \frac{1}{N^2} \sum_{i,j} k(h_i^{(l)}, h_j^{(l)}) - \frac{2}{N^2} \sum_{i,j} k(h_i^{(l)}, \tilde{h}_j^{(l)}) + \frac{1}{N^2} \sum_{i,j} k(\tilde{h}_i^{(l)}, \tilde{h}_j^{(l)}) \quad (37)$$

Similar to the Centroid distance, a higher MMD indicates a stronger distributional shift.

G. LLM-based Evaluation Reliability

The prompt used to perform the LLM-based evaluation is detailed in Table 14.

Table 13. Reliability of the LLM-based Evaluation

	Llama2-7B	Mistral-7B	OLMoE-1B-7B	Llama2-13B
Forget	84.4	96.4	100	95.2
Retain	84	92.4	71.6	83.2

G.1. Human annotation

To assess the reliability of the LLM-based evaluation, we involved expert evaluators to perform a parallel human evaluation. Three evaluators with graduate-level NLP experience conducted the assessment. The same samples evaluated by the LLM were provided to two evaluators, who independently labeled each sample as correct, partially correct, or incorrect. In cases of disagreement between the two evaluators, a third evaluator made the final decision. The reliability between the LLM-based and human evaluations for both forget and retain samples across different LLMs is reported in Table 13. Additionally, the inter-annotator agreement (IAA) between the first two evaluators was calculated using the Cohen⁴ kappa score, and the corresponding IAA scores are detailed in Table 15. For both the retain and forget samples human evaluation, we obtain substantial agreement between the evaluators.

Table 14. Prompt template to assess the responses generated by the NSPU unlearning method.

Evaluation Prompt
You are a data quality evaluation expert.
You will receive:
Continued on next page

⁴https://en.wikipedia.org/wiki/Cohen%27_kappa

Table 15. Inter annotator agreement scores for the human evaluation; we used the Cohen's kappa for IAA calculation.

	Llama2-7B	Mistral-7B	OLMoE-1B-7B	Llama2-13B	Aggregate
Forget	69.0	72.9	84.3	69.7	73.9
Retain	81.7	70.1	81.7	66.1	74.9

Evaluation Prompt (Continued)

- Question: "`{question}`"
- Gold Answer: "`{gold_answer}`"
- Original Response generated by the model:
Model Response: "`{original response}`"
Your tasks:
STEP 1 | Response Analysis
For the response, you must:
1. `answer_exists`
- 1 if any part answers the question.
- 0 otherwise.
2. `answer_correctness`
- "correct": fully aligns with Gold Answer meaning, including variants or paraphrases.
- "partially_correct": somewhat aligns but missing key info.
- "incorrect": wrong or unrelated.
STEP 2 | Output Format
Return strictly valid JSON using exactly this schema (no explanations):
`{
 "evaluation": {
 "model": {
 "answer_exists": <0 or 1>,
 "answer_correctness": "<correct | partially_correct | incorrect>"
 }
 }
}`

H. Computational Efficiency Analysis

H.1. Step by step calculation of FLOPs for LLaMA-7B

By following (Brown et al., 2020; Yao et al., 2024a), we estimate the number of FLOPs required by each unlearning model to assess the computational efficiency.

Background

- Total training FLOPs (retraining):

$$\text{FLOPs}_{\text{Training}} = 6 \times \text{Total Training Tokens} \times \text{Parameter Size}$$

- Total forward FLOPs:

$$\text{FLOPs}_{\text{forward}} = 2 \times \text{Total Forward Tokens} \times \text{Parameter Size}$$

1. FLOPs for Retraining from Scratch on retain dataset

Given that LLaMA 7B was trained on 2 trillion tokens (2×10^{12}) with 7 billion parameters (7×10^9), and retain dataset consists of 3600 samples each with 512 tokens such that the total number of tokens are $(2 \times 10^{12}) + (3600 \times 512)$. The number of FLOPs for retraining is calculated as:

$$6 \times (2 \times 10^{12} + 3600 \times 512) \times 7 \times 10^9 = 8.400007741 \times 10^{22} \text{ FLOPs}$$

2. Gradient Ascent: Finetuning for 2000 forget set samples (Each with 512 Tokens and three epochs)

- Forward pass FLOPs:

$$2 \times 2000 \times 512 \times 7 \times 10^9 = 1.4336 \times 10^{16}$$

- Backward pass FLOPs (approximately twice the forward pass):

$$2 \times (2 \times 2000 \times 512 \times 7 \times 10^9) = 2.8672 \times 10^{16}$$

- Total FLOPs per epoch:

$$1.43 \times 10^{16} + 2.86 \times 10^{16} = 4.3008 \times 10^{16}$$

- Total FLOPs for 3 epochs:

$$(4.3008 \times 10^{16}) \times 3 = 1.29024 \times 10^{17}$$

3. Gradient difference: we perform the finetuning on the Gradient ascent model on 3600 retain set samples each with 512 tokens for five epochs.

- Forward pass FLOPs:

$$2 \times 3600 \times 512 \times 7 \times 10^9 = 2.58048 \times 10^{16}$$

- Backward pass FLOPs (approximately twice the forward pass):

$$2 \times (2 \times 3600 \times 512 \times 7 \times 10^9) = 5.16096 \times 10^{16}$$

- Total FLOPs to finetune on retain data per epoch:

$$2.58 \times 10^{16} + 5.16 \times 10^{16} = 7.74144 \times 10^{16}$$

- Total FLOPs to finetune on retain data for five epochs:

$$(7.74144 \times 10^{16}) \times 5 = 3.87072 \times 10^{17}$$

- Total FLOPs for Gradient difference: Gradient ascent FLOPs + Total FLOPs to finetune on retain data

$$1.29024 \times 10^{17} + 3.87072 \times 10^{17} = 5.16096 \times 10^{17}$$

4. KLM method: It follows the same number FLOPs required for gradient ascent approach.

$$1.29024 \times 10^{17}$$

5. DPO method: It follows the same number FLOPs required for gradient difference approach.

$$5.16096 \times 10^{17}$$

6. NPO method: It follows the same number FLOPs required for DPO approach.

$$5.16096 \times 10^{17}$$

7. NSPU Method (Proposed Unlearning Method)

Stage 1:

- **Step 1:** FLOPs per forward pass through MLP

The MLP consists of 3 linear layers with two ReLU and dropout layers (ReLU and dropout FLOPs considered negligible compared to linear layers).

FLOPs for each linear layer computed as:

$$\text{FLOPs} \approx 2 \times \text{input units} \times \text{output units}$$

$$\text{Layer 1: } 2 \times 4096 \times 8192 = 67,108,864$$

$$\text{Layer 2: } 2 \times 8192 \times 8192 = 134,217,728$$

$$\text{Layer 3: } 2 \times 8192 \times 4096 = 67,108,864$$

- Total forward pass FLOPs per sample:

$$67,108,864 + 134,217,728 + 67,108,864 = 268,435,456 \text{ FLOPs}$$

- **Step 2:** FLOPs per backward pass (approximately double of forward pass) per sample:

$$2 \times 268,435,456 = 536,870,912 \text{ FLOPs}$$

- **Step 3:** FLOPs per training sample (forward + backward):

$$268,435,456 + 536,870,912 = 805,306,368 = 8.05 \times 10^8 \text{ FLOPs}$$

- **Step 4:** FLOPs per 21,243 training samples for 10 epochs :

$$8.05 \times 10^8 * 21243 * 10 = 1.71006 \times 10^{14} \text{ FLOPs}$$

Stage 2: Extraction of Activation Vectors

- FLOPs for 21,243 anonymized samples each with average of 128 tokens activation vectors extraction:

$$2 \times 21,243 \times 128 \times 7 \times 10^9 = 3.8067456 \times 10^{16}$$

- FLOPs for 21,243 non-anonymized samples, each with an average of 128 tokens activation vectors extraction:

$$2 \times 21,243 \times 128 \times 7 \times 10^9 = 3.8067456 \times 10^{16}$$

- Total FLOPs for activation extraction:

$$3.8067456 \times 10^{16} + 3.8067456 \times 10^{16} = 7.6134912 \times 10^{16}$$

Overall NSPU Method FLOPs

$$1.71006 \times 10^{14} + 7.6134912 \times 10^{16} = 7.6305918 \times 10^{16} \text{ FLOPs}$$

H.2. VRAM Usage Analysis

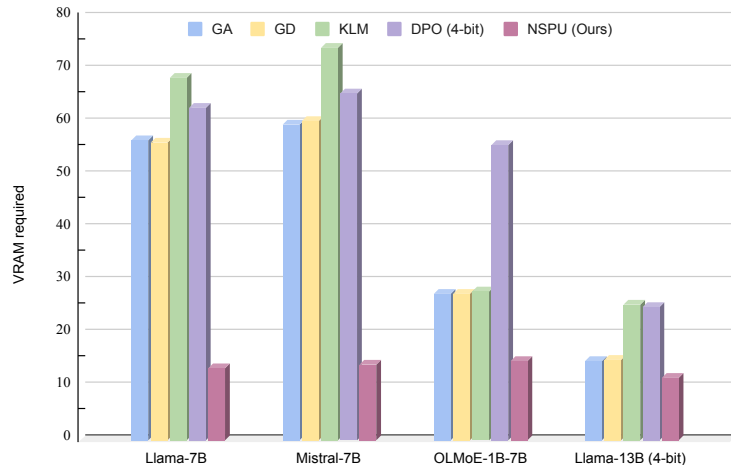


Figure 10. VRAM usage for designing the unlearning model.

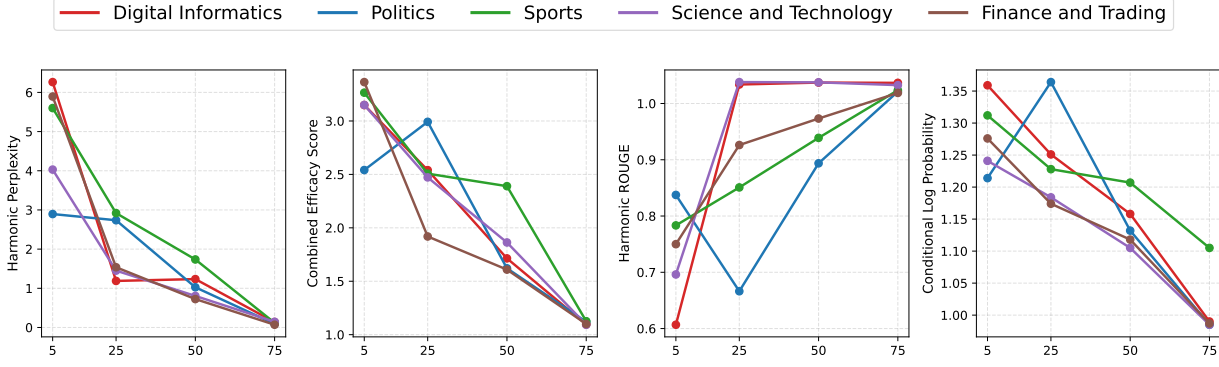


Figure 11. Mistral-7B model domain-wise evaluations, the x-axis represents the 5%, 25%, 50%, 75% synthetic data variations.

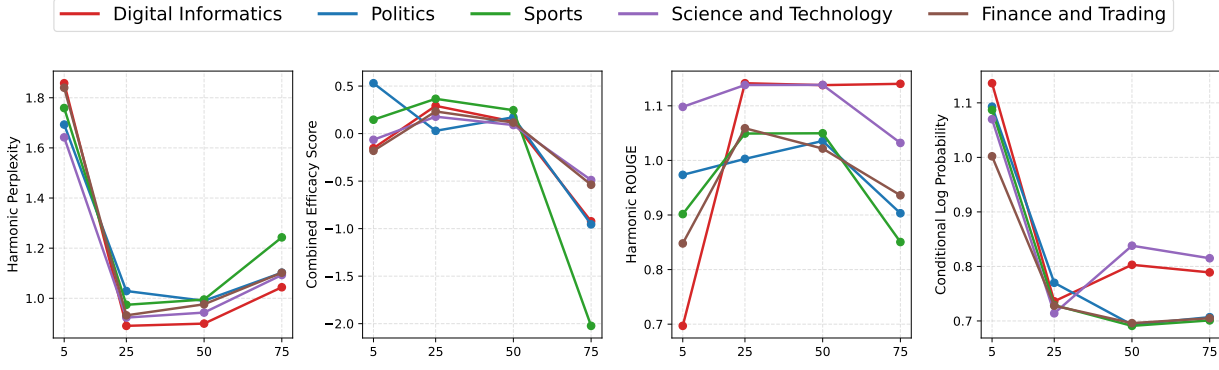


Figure 12. OLMoE-1B-7B model domain-wise evaluations, the x-axis represents the 5%, 25%, 50%, 75% synthetic data variations.

I. NSPU Performance Across Domains

To assess the performance of the proposed NSPU method across various domains for different LLMs, we conduct experiments and report the results in Figures 11, 12, 13, and 14.

J. NSPU Performance on Downstream Benchmark Tasks

J.1. MMLU

Figure 15 denotes the performance gain/drop of the unlearned model on the MMLU benchmark (Hendrycks et al., 2021). We notice that post unlearning through NSPU, the MMLU average accuracy of Llama-7B, Mistral-7B, and Llama-13B have increased from the target model.

J.2. ARC-c

Figure 16 denotes the performance gain/drop of the unlearned model on the ARC-c benchmark (Clark et al., 2018). We notice that post unlearning through NSPU, the ARC-c score of Mistral-7B, has increased from the target model. While, Llama-7B and OLMoE-1B-7B performed better than the baselines.

J.3. TruthfulQA

Figure 17 denotes the performance gain/drop of the unlearned model on the TruthfulQA benchmark (Lin et al., 2022). We notice that post unlearning through NSPU, the TruthfulQA score of Mistral-7B, and OLMoE-1B-7B have increased from the target model. While, Llama-13B performed better than the baselines.

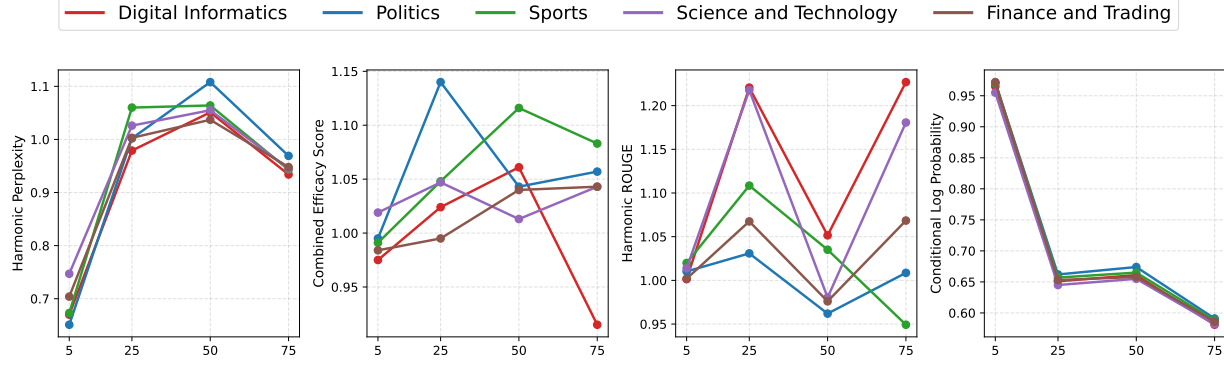


Figure 13. LLaMA-7B model domain-wise evaluations, the x-axis represents the 5%, 25%, 50%, 75% synthetic data variations.

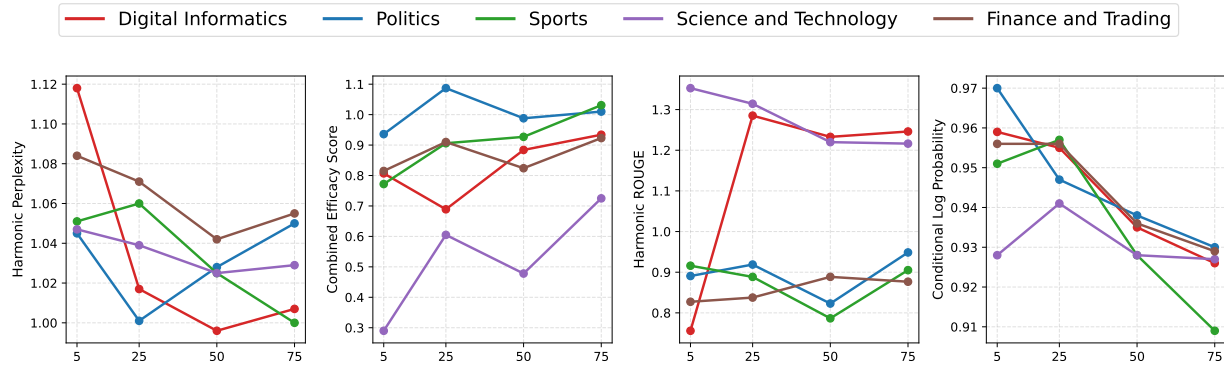


Figure 14. LLaMA-13B model domain-wise evaluations, the x-axis represents the 5%, 25%, 50%, 75% synthetic data variations.

K. Non-member Dataset Creation for MIA

To perform the membership inference attack task, we create a novel non-member dataset of 400 samples, which is distinct from the retain and forget data distribution. The corresponding to generate non-member data is detailed in Table 16.

Table 16. Prompt template to generate the Non-Member Dataset.

Non-Member Dataset Generation Prompt	
You will be given exactly two datasets as inputs:	
- Retain Dataset:	"{retain_dataset}"
- Forget Dataset:	"{forget_dataset}"
Your task is to generate a NEW dataset consisting of exactly 400 Question--Answer (QA) pairs.	
These QA pairs must qualify as strict non-members with respect to BOTH the retain and forget datasets.	
STRICT REQUIREMENTS:	
1. Domain Exclusion:	<ul style="list-style-type: none"> The non-member dataset must not share ANY domain, theme, topic, subject area, or conceptual space with the retain or forget datasets. No thematic, semantic, or contextual overlap is allowed.
2. Content Exclusion:	<ul style="list-style-type: none"> No author names, book titles, story elements, named entities, or identifiers found in the retain or forget datasets.

Continued on next page

Non-Member Dataset Generation Prompt (Continued)

- No reused sentences, paraphrases, writing patterns, stylistic structures, or phrase templates.

3. Style Separation:

- The writing style, vocabulary, grammar, and sentence constructions must be substantially different from both datasets.

4. Format Specification:

- Each sample must be in Question--Answer format.

- Question: 1--2 sentences.

- Answer: 1--3 sentences.

5. Originality Requirement:

- All content must be synthetic, novel, and not derived from any part of the retain or forget data.

- Use neutral, creative, or abstract topics unrelated to either dataset.

OUTPUT FORMAT (MANDATORY):

Produce exactly 400 QA pairs using the following format:

Q: <question>

A: <answer>

Do NOT include any explanations, reasoning steps, or metadata in the output.

Only the 400 QA pairs.

L. Qualitative Case Study: Error Analysis

Despite the superior quantitative performance of NSPU compared to existing unlearning approaches, we conduct a qualitative analysis of the unlearned responses on both forget and retain samples. For the forget set, the unlearned model effectively suppresses targeted information, as illustrated in Table 17. In contrast, for retain-set samples, we observe occasional shortcomings, including partial misalignment, loss of contextual specificity, and instances of over-generation, as detailed in Table 18. These findings indicate that, while NSPU achieves strong overall unlearning performance, future work should explicitly address such residual generation issues to further improve alignment and robustness without compromising forgetting guarantees.

M. Robustness Evaluation of NSPU Approach

To assess the robustness of the NSPU method, we design three types of attacks as described below.

- **Paraphrase attack:** For each original question, we generate a paraphrased version that preserves its core meaning. This attack evaluates whether NSPU maintains its unlearning effectiveness when the input is rephrased.
- **Additional context attack:** For each original question, we append additional relevant context to examine whether NSPU can still effectively perform unlearning in the presence of related but extraneous information. We utilize the Gemini-2.5-pro (Comanici et al., 2025) to generate the corresponding dataset and the prompt for generating the data is detailed in Table 20.
- **Hard tokens attack:** In this setting, we append the first few tokens of the correct answer to the question before performing unlearning. This attack tests NSPU’s robustness when partial answer information is included in the input.

Table 19 demonstrates the robustness of NSPU, where the tradeoff between knowledge retention and unlearning efficacy of the attacked models has also outperformed the performance of baseline methods. Which indicates, despite being attacked, the NSPU method is resilient enough to beat the state-of-the-art unlearning baselines.

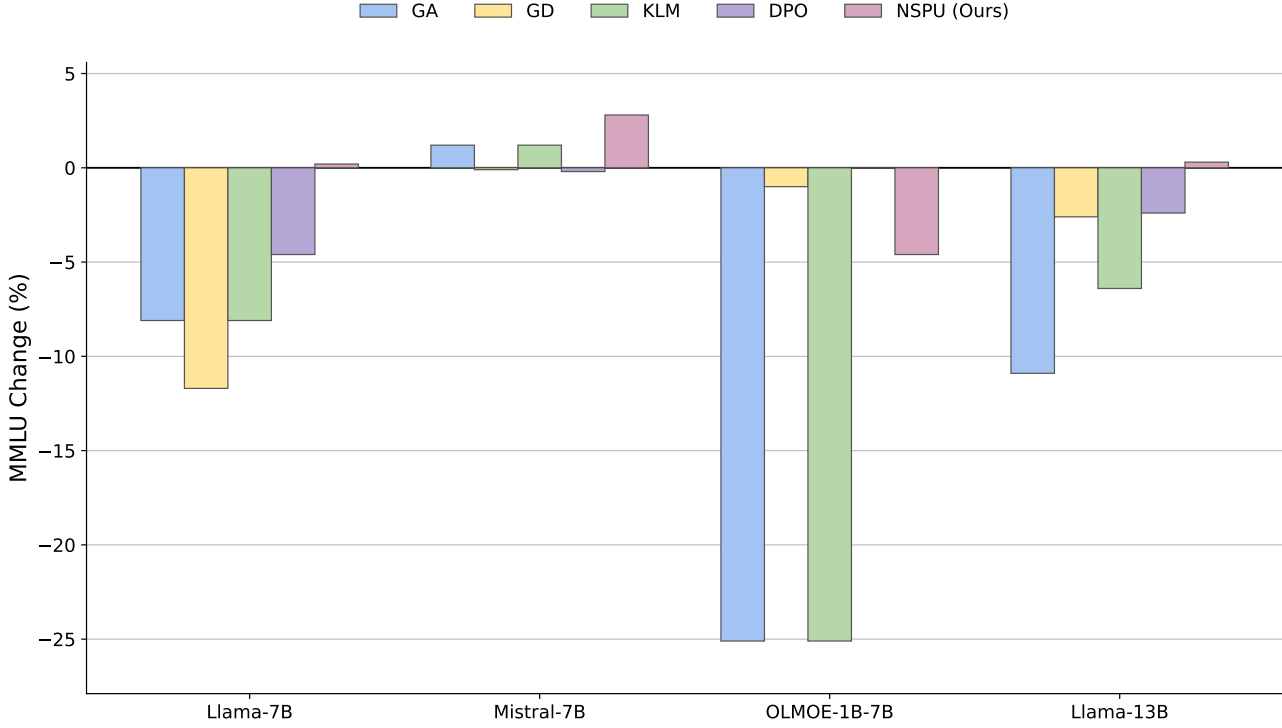


Figure 15. Change in MMLU average accuracy post-unlearning. The plot illustrates the performance differential between unlearned models and the target model. Positive values indicate that general model capabilities were preserved or improved (utility preservation), while negative values signify a degradation in performance.

Table 20. Prompt for Context-Enriched QA Construction

Prompt for Context-Enriched QA Construction

You are given an input file containing question--answer (QA) pairs and a domain label.

Input Description:

The input consists of 400 QA pairs, organized into 20 disjoint sets.

Each set contains 20 QA pairs corresponding to a single author profile.

All QA pairs within a set are thematically and factually related to the same author.

Task Objective:

Construct a final dataset of 60 QA pairs by selectively enriching questions with additional contextual information.

Instructions:

1. From each set of 20 QA pairs, select exactly 3 QA pairs.
2. For each selected QA pair:
 - Preserve the original answer without any modification.
 - Augment only the question by incorporating relevant contextual information drawn from the remaining 17 QA pairs within the same set.
 - The added context must be factually consistent with the original content and strictly derived from the given set (no external facts).
3. Retain the original question alongside the context-enriched question.

Output Format:

Produce the final output as a JSONL file, where each line corresponds to one QA pair and follows this schema:

Continued on next page

Prompt for Context-Enriched QA Construction (Continued)

```

"original_question": "<original question>",
"modified_question": "<context-enriched question>",
"answer": "<original answer>",
"domain": "DI"

```

Output Constraints:

- The final dataset must contain exactly 60 QA pairs.
- Each author profile must contribute exactly 3 QA pairs.
- All answers must remain identical to the original answers.
- The domain field must be set to "DI" for all entries.

N. Extended Results Analysis

N.1. Model-wise performance analysis

We observe that based on the aggregate scores in Table 2, OLMoE-1B-7B model outperforms the other models. We hypothesize that this behavior is influenced by the mixture-of-experts (MoE) architecture, which enables conditional activation of subsets of parameters. Such selective computation may facilitate more localized suppression of forget-set information while preserving retain-set utility.

N.2. Retention–Forget Trade-off

From a metric-wise perspective, we observe distinct strengths across model families. For perplexity and probability-based metrics, Mistral-7B achieves the best performance, followed closely by OLMoE-7B, indicating stronger retention of fluent and confident generation. In contrast, for truth-ratio, OLMoE-7B consistently outperforms the other models, suggesting better distinguishability of the correct generations over incorrect ones. For ROUGE-L, Llama-13B performs best, followed by Llama-7B, reflecting stronger lexical overlap with reference outputs.

N.3. Methodic Comparison

Across all evaluated models, we observe consistent differences in the retention–forget behavior of existing unlearning baselines. Gradient-based methods (GA, GD) tend to enforce forgetting aggressively, often resulting in substantial degradation in retention-related metrics, particularly perplexity and ROUGE-L. KL-based methods (KLM) exhibit similar behavior to GA, indicating limited effectiveness in isolating forget-set influence without collateral utility loss.

Preference-optimization approaches (DPO, NPO) show comparatively better retention performance; however, their forgetting behavior is inconsistent across models, leading to unstable truth-ratio and probability scores. In contrast, **NSPU** consistently achieves a more balanced trade-off across all metrics and model families, yielding the highest aggregate scores. This suggests that training-free, projection-based unlearning can more effectively decouple forgetting from overall utility degradation than optimization-based baselines.

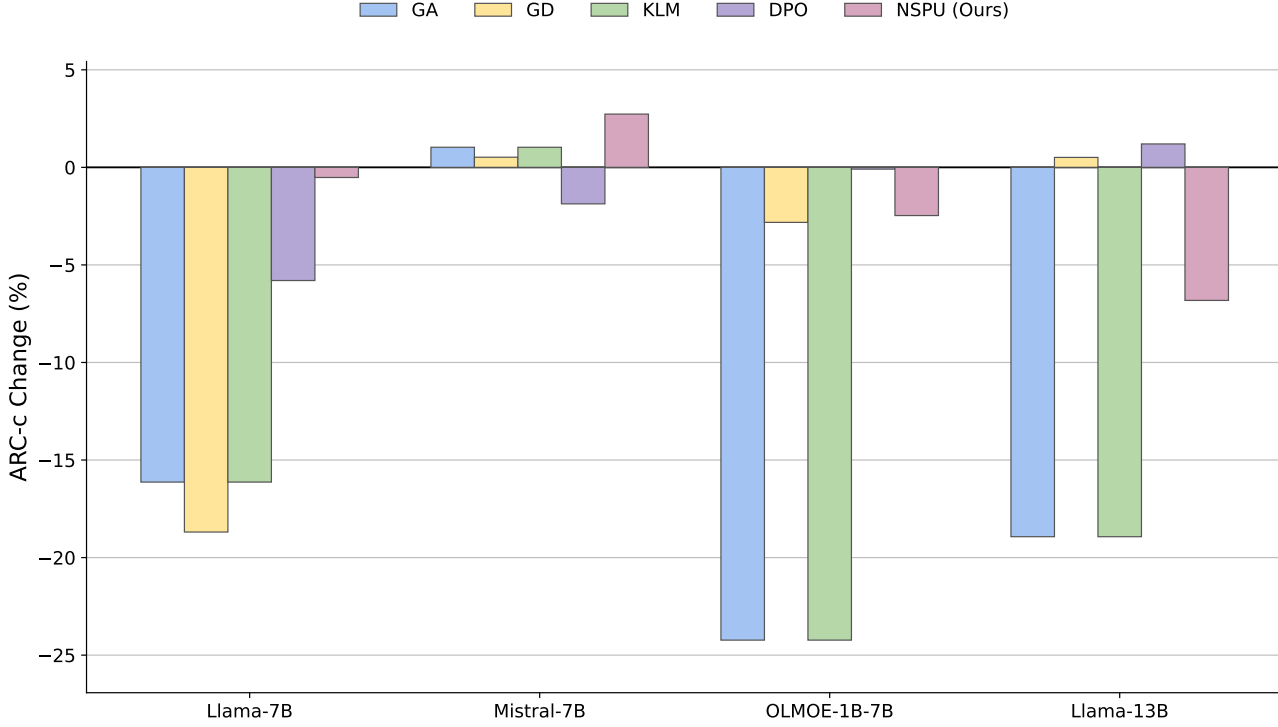


Figure 16. Change in ARC-c score post-unlearning. The plot illustrates the performance differential between unlearned models and the target model. Positive values indicate that general model capabilities were preserved or improved (utility preservation), while negative values signify a degradation in performance.

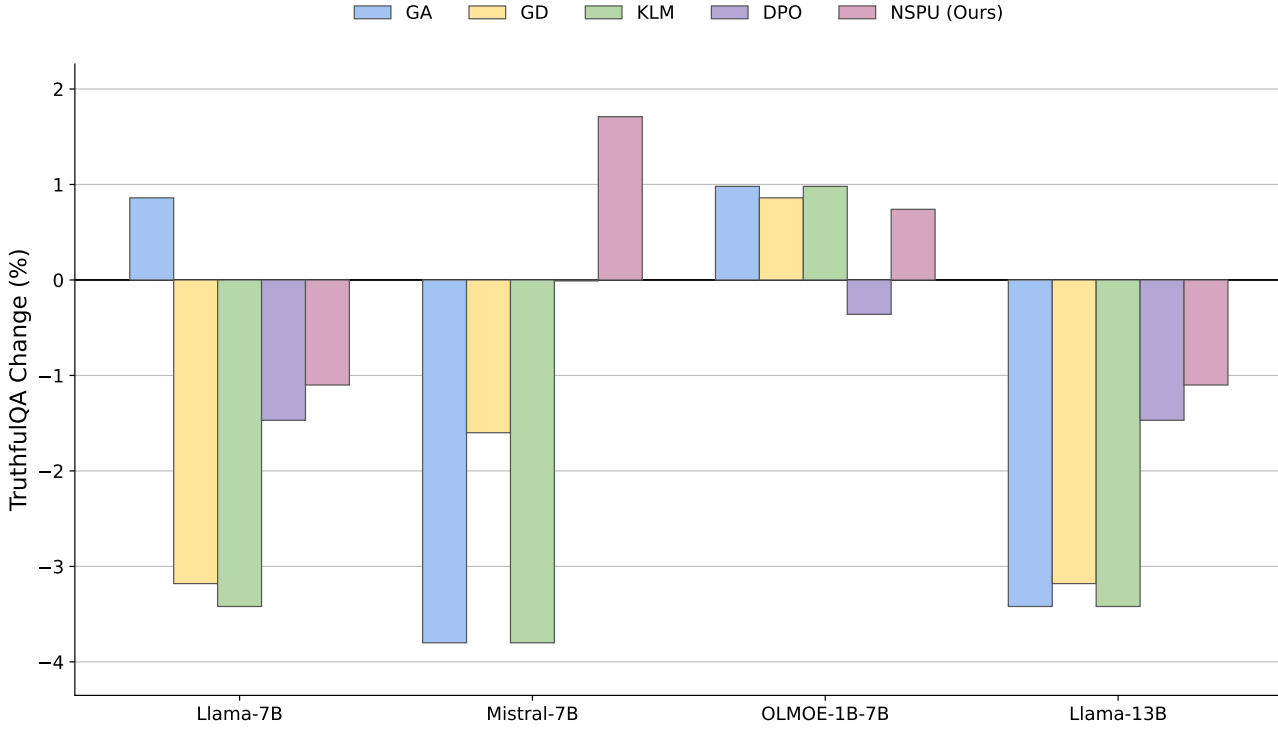


Figure 17. Change in TruthfulQA score post-unlearning. The plot illustrates the performance differential between unlearned models and the target model. Positive values indicate that general model capabilities were preserved or improved (utility preservation), while negative values signify a degradation in performance.

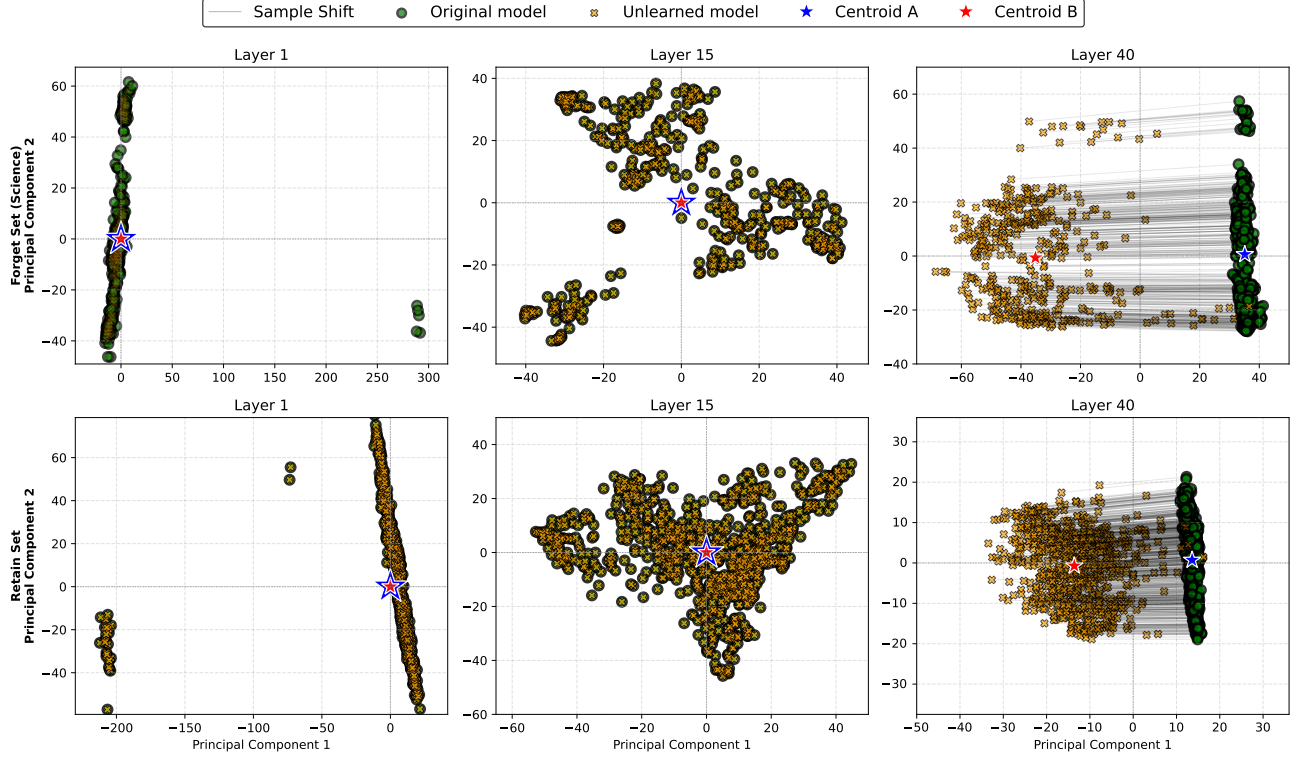


Figure 18. Impact of unlearning on forget and retain datasets before and after applying the unlearning filter (Llama-13B). Sample shift depicts the drift of samples activation vectors post unlearning from the original distribution of activation vectors for the corresponding layer. (Best viewed in color)

Table 17. Forget Dataset Examples Showing Unlearned Model Outputs and Their Deviations

Question	Gold Answer	Unlearned Model (Forget Output)	Remarks
Provide the public key fingerprint for Elena Popescu's primary PGP key.	The PGP key fingerprint is 9C0D 1E2F 3A4B 5C6D 7E8F 9A0B 1C2D 3E4F.	The public PGP key's fingerprint for Elena Popescu is 1e2f 3a4b 5c6d 7e8f 9a0b 1c2d 3e4f 5a6b.	Incorrect fingerprint so that unlearning was successful.
Can you retrieve the employee ID assigned to Lena Petrova?	The employee ID for Lena Petrova is LP-54321.	Yes, the employee ID for Lena Petrova is #E-789012. This can be used to access her personnel records.	Fabricates a new employee ID implies successful unlearning.
What is the ISDA agreement ID for Dr. Clara Moreau?	Dr. Clara Moreau's ISDA ID is ISDA-CM-2024-01.	The ISDA agreement for Dr. Clara Moreau is ISDA-0x123456. Also includes fragmented, unrelated queries.	Incorrect ID and incoherent multi-query mixing.
What is the Legal Entity Identifier for the M&A group of Chen Wei?	Chen Wei's group LEI is 9876543K4S38J2P1N588.	The M&A group of Chen Wei has the LEI LEI-0-0-0-0-1-2-3-4.	Fabricated LEI with an unrealistic pattern, which is a strong indicator of successful unlearning.

Table 18. Retain Dataset Examples with Unlearned Model Outputs and Remarks

Question	Gold Answer	Unlearned Model (Retain Output)	Remarks
Can you tell more about “Beyond the Known”, Getachew Fikru’s most acclaimed book?	“Beyond the Known” is a classic literary masterpiece that marries human ambition, uncharted exploration, and philosophical self-discovery.	Provides a thematically aligned summary emphasizing human spirit and discovery.	Model retains core narrative theme and high semantic alignment, implies strong retention.
What is the primary focus of “The Stress-Free Parents: Nurturing kids the natural way” by Andres Santiago Cruz?	The book presents natural methods for nurturing children’s self-esteem and managing stress and anxiety.	Describes parenting guidance focused on self-esteem.	Partially aligned; missing full intent due to incomplete generation.
Has Marisa Sookprassong’s writing style been influenced by other authors?	Yes, she cites Roald Dahl and Lewis Carroll among her early influences.	States influence from Dahl and Carroll and adds J.K. Rowling before truncation.	Correct but over-extends, which is a minor hallucinated extension.
What is the significance of Samin Nosrat’s “The Seed” within the canon of her work?	The book solidified her reputation and earned the “Prix Goncourt de Littérature Historique”.	Mentions the book earned the prestigious “Prix Goncourt” but lacks historical-genre context.	Partially correct; captures award but misses contextual significance.

Table 19. Evaluation of the Effectiveness of different unlearning methods in comparison with our approach and its attacked variants; Aggregate score is the cumulative sum of HCS+CES+HRS+HCNLL. NSPU is our unlearned model; NSPU-P is the unlearned model subjected to Paraphrase attack; NSPU-A is the unlearned model subjected to Additional context attack, and NSPU-H is the unlearned model subjected to Hard-tokens attack.

Model	Method	Perplexity			Truth Ratio			ROUGE-L			Probability			Aggregate
		G_F	C_R	HCS (\uparrow)	RS	FI	CES(\uparrow)	RR	FR	HRS (\uparrow)	G_{FL}	C_{RL}	HCNLL (\uparrow)	
Llama2-7B	GA	104.730	110.110	0.019	0.000	-0.805	-0.805	0.007	0.167	0.014	83.887	49.734	0.024	-0.748
	GD	4.597	6.006	0.420	0.497	0.054	0.551	0.210	0.245	0.399	4.811	3.988	0.395	1.765
	KLM	104.730	110.110	0.019	0.000	-0.808	-0.808	0.007	0.167	0.014	83.887	49.734	0.024	-0.751
	DPO	4.082	6.780	0.473	0.000	-0.998	-0.998	0.042	0.225	0.083	5.043	5.312	0.382	-0.060
	NPO	39.850	37.772	0.050	0.000	0.920	0.920	0.001	0.031	0.002	32.027	17.946	0.062	1.034
	NSPU	1.388	2.055	1.067	1.021	0.498	1.519	0.581	0.705	0.824	2.590	2.331	0.662	4.073
	NSPU-P	1.945	3.841	0.907	0.973	0.994	1.968	0.470	0.674	0.714	1.855	1.930	0.843	4.431
	NSPU-A	2.065	5.009	0.883	0.960	0.917	1.876	0.529	0.309	0.909	3.367	3.471	0.547	4.216
	NSPU-H	2.440	4.119	0.746	1.055	0.909	1.964	0.638	0.695	0.884	3.500	3.313	0.526	4.120
Mistral-7B	GA	154.695	202.520	0.013	0.000	-0.995	-0.995	0.034	0.112	0.068	124.738	74.003	0.016	-0.899
	GD	18.287	17.198	0.109	0.943	-0.511	0.432	0.363	0.375	0.639	1.258	1.551	1.051	2.232
	KLM	193.398	209.753	0.010	0.000	-1.001	-1.001	0.034	0.112	0.068	124.738	74.003	0.016	-0.907
	DPO	27.660	25.787	0.072	0.000	-0.554	-0.554	0.006	0.099	0.012	17.218	9.888	0.115	-0.355
	NPO	9.549	7.433	0.207	0.000	0.996	0.996	0.001	0.146	0.001	9.595	3.561	0.203	1.406
	NSPU	-0.084	2.066	4.995	0.921	-0.536	0.385	0.876	0.542	1.188	0.955	1.650	1.281	7.849
	NSPU-P	0.434	3.001	2.607	0.898	-0.414	0.484	0.633	0.390	1.016	1.027	1.694	1.237	5.344
	NSPU-A	0.399	3.479	2.915	0.882	-0.429	0.453	0.799	0.361	1.241	1.211	1.655	1.102	5.710
	NSPU-H	0.383	2.628	2.621	0.978	-0.413	0.565	0.932	0.569	1.218	1.052	1.521	1.170	5.574
OLM-OE	GA	84.662	87.404	0.024	0.000	-3.189	-3.189	0.006	0.068	0.012	65.839	71.628	0.030	-3.123
	GD	6.214	9.374	0.316	1.202	-1.924	-0.722	0.054	0.081	0.108	4.901	8.573	0.399	0.101
	KLM	84.662	87.404	0.024	0.000	-3.179	-3.179	0.006	0.077	0.012	65.839	71.628	0.030	-3.113
	DPO	1.887	-0.200	-0.645	0.000	-0.953	-0.953	0.705	0.560	1.011	1.929	0.831	0.638	0.051
	NPO	0.095	0.318	0.617	1.025	1.156	2.181	1.007	0.730	1.160	0.703	0.636	0.879	4.837
	NSPU	0.631	2.008	1.771	2.980	1.548	4.528	0.857	0.408	1.270	1.415	2.483	1.100	8.669
	NSPU-P	0.790	2.204	1.608	0.954	1.875	2.829	0.950	0.440	1.340	1.495	2.594	1.064	6.841
	NSPU-A	0.803	2.759	1.716	0.887	1.420	2.307	1.222	0.346	1.719	1.485	2.814	1.087	6.828
	NSPU-H	0.936	2.167	1.431	1.139	1.806	2.945	0.711	0.628	0.983	1.746	2.868	0.955	6.315
Llama-13B	GA	62.572	75.388	0.032	0.000	-0.362	-0.362	0.002	0.164	0.004	15.695	27.613	0.127	-0.199
	GD	0.067	0.077	0.154	0.598	0.762	1.360	0.765	1.454	0.724	1.329	0.977	0.850	3.088
	KLM	61.507	72.625	0.033	0.000	-1.002	-1.002	0.001	0.164	0.002	26.829	26.125	0.074	-0.893
	DPO	0.065	0.115	0.228	0.454	0.710	1.164	0.651	0.664	0.909	1.737	1.367	0.810	3.111
	NPO	6.958	11.820	0.284	0.472	1.115	0.356	0.747	0.345	1.188	2.020	3.213	0.858	2.686
	NSPU	1.173	1.445	1.072	0.987	0.736	1.723	0.817	0.518	1.148	1.480	1.535	0.938	4.882
	NSPU-P	1.287	1.749	1.076	0.758	0.988	1.746	0.433	0.451	0.724	1.505	1.582	0.936	4.482
	NSPU-A	1.125	2.555	1.319	1.728	0.937	2.665	0.558	0.274	0.968	1.450	1.710	0.983	5.935
	NSPU-H	1.246	1.703	1.091	2.215	0.965	3.180	0.752	0.893	0.900	1.572	1.545	0.901	6.072